

September 2016

## **A Bat-Derived Putative Cross-Family Recombinant Coronavirus with a Reovirus Gene**

Canping Huang

William J. Liu

Wen Xu

Follow this and additional works at: [https://digitalcommons.usf.edu/kip\\_articles](https://digitalcommons.usf.edu/kip_articles)

---

### **Recommended Citation**

Huang, Canping; Liu, William J.; and Xu, Wen, "A Bat-Derived Putative Cross-Family Recombinant Coronavirus with a Reovirus Gene" (2016). *KIP Articles*. 396.  
[https://digitalcommons.usf.edu/kip\\_articles/396](https://digitalcommons.usf.edu/kip_articles/396)

This Article is brought to you for free and open access by the KIP Research Publications at Digital Commons @ University of South Florida. It has been accepted for inclusion in KIP Articles by an authorized administrator of Digital Commons @ University of South Florida. For more information, please contact [digitalcommons@usf.edu](mailto:digitalcommons@usf.edu).

RESEARCH ARTICLE

# A Bat-Derived Putative Cross-Family Recombinant Coronavirus with a Reovirus Gene

Canping Huang<sup>1</sup>✉, William J. Liu<sup>1,2</sup>✉, Wen Xu<sup>3</sup>✉, Tao Jin<sup>4</sup>✉, Yingze Zhao<sup>1</sup>, Jingdong Song<sup>1</sup>, Yi Shi<sup>5</sup>, Wei Ji<sup>1</sup>, Hao Jia<sup>1,2</sup>, Yongming Zhou<sup>3</sup>, Honghua Wen<sup>6</sup>, Honglan Zhao<sup>1</sup>, Huaxing Liu<sup>6</sup>, Hong Li<sup>3</sup>, Qihui Wang<sup>7</sup>, Ying Wu<sup>5</sup>, Liang Wang<sup>5</sup>, Di Liu<sup>5,8</sup>, Guang Liu<sup>4</sup>, Hongjie Yu<sup>9</sup>, Edward C. Holmes<sup>10</sup>, Lin Lu<sup>3\*</sup>, George F. Gao<sup>1,2,5,11,12,13\*</sup>



## OPEN ACCESS

**Citation:** Huang C, Liu WJ, Xu W, Jin T, Zhao Y, Song J, et al. (2016) A Bat-Derived Putative Cross-Family Recombinant Coronavirus with a Reovirus Gene. PLoS Pathog 12(9): e1005883. doi:10.1371/journal.ppat.1005883

**Editor:** Susan Baker, Loyola, UNITED STATES

**Received:** May 1, 2016

**Accepted:** August 19, 2016

**Published:** September 27, 2016

**Copyright:** © 2016 Huang et al. This is an open access article distributed under the terms of the [Creative Commons Attribution License](https://creativecommons.org/licenses/by/4.0/), which permits unrestricted use, distribution, and reproduction in any medium, provided the original author and source are credited.

**Data Availability Statement:** The complete genome sequences of Ro-BatCoV GCCDC1 strains 346 and 356 have been deposited in the GenBank database and assigned accession numbers KU762337 and KU762338, respectively (<http://www.ncbi.nlm.nih.gov/nuccore/KU762337> and <http://www.ncbi.nlm.nih.gov/nuccore/KU762338>). We also deposited the sequences of the p10 genes from the rectal swabs of 24 bats in GenBank. All these accession numbers are listed in [S8 Table](#).

**Funding:** This work was supported by the National Natural Science Foundation of China (NSFC) Grant No. 81290342 and 81461168030 (to GFG), and Grant No. 81373141 and 81401312 (to WJL), the China

**1** National Institute for Viral Disease Control and Prevention, Chinese Center for Disease Control and Prevention (China CDC), Beijing, China, **2** College of Laboratory Medicine and Life Sciences, Wenzhou Medical University, Wenzhou, China, **3** Yunnan Provincial Center for Disease Control and Prevention, Kunming Yunnan, China, **4** China National Genebank-Shenzhen, BGI-Shenzhen, Shenzhen, China, **5** CAS Key Laboratory of Pathogenic Microbiology and Immunology, Institute of Microbiology, Chinese Academy of Sciences, Beijing, China, **6** Center for Disease Control and Prevention of Mengla County, Mengla Yunnan, China, **7** CAS Key Laboratory of Microbial and Metabolic Engineering, Institute of Microbiology, Chinese Academy of Sciences, Beijing, China, **8** Network Information Center, Institute of Microbiology, Chinese Academy of Sciences, Beijing, China, **9** Division of Infectious Disease, Key Laboratory of Surveillance and Early-warning on Infectious Disease, Chinese Centre for Disease Control and Prevention, Beijing, China, **10** Marie Bashir Institute of Infectious Diseases and Biosecurity, Charles Perkins Centre, School of Biological Sciences and Sydney Medical School, The University of Sydney, Sydney, New South Wales, Australia, **11** Laboratory of Protein Engineering and Vaccines, Tianjin Institute of Industrial Biotechnology, Chinese Academy of Sciences, Tianjin, China, **12** Research Network of Immunity and Health (RNIH), Beijing Institutes of Life Science, Chinese Academy of Sciences, Beijing, China, **13** Office of Director-General, Chinese Center for Disease Control and Prevention (China CDC), Beijing, China

✉ These authors contributed equally to this work.

\* [lulin@yncdc.cn](mailto:lulin@yncdc.cn) (LL); [gaofu@chinacdc.cn](mailto:gaofu@chinacdc.cn) (GFG)

## Abstract

The emergence of severe acute respiratory syndrome coronavirus (SARS-CoV) in 2002 and Middle East respiratory syndrome coronavirus (MERS-CoV) in 2012 has generated enormous interest in the biodiversity, genomics and cross-species transmission potential of coronaviruses, especially those from bats, the second most speciose order of mammals. Herein, we identified a novel coronavirus, provisionally designated Roussettus bat coronavirus GCCDC1 (Ro-BatCoV GCCDC1), in the rectal swab samples of *Roussettus leschenaulti* bats by using pan-coronavirus RT-PCR and next-generation sequencing. Although the virus is similar to Roussettus bat coronavirus HKU9 (Ro-BatCoV HKU9) in genome characteristics, it is sufficiently distinct to be classified as a new species according to the criteria defined by the International Committee of Taxonomy of Viruses (ICTV). More striking was that Ro-BatCoV GCCDC1 contained a unique gene integrated into the 3'-end of the genome that has no homologs in any known coronavirus, but which sequence and phylogeny analyses indicated most likely originated from the p10 gene of a bat orthoreovirus. Sub-genomic mRNA and cellular-level observations demonstrated that the p10 gene is functional and induces the formation of cell syncytia. Therefore, here we report a putative heterologous inter-family recombination event between a single-stranded, positive-sense

National Grand S&T Special Project Grant No. 2014ZX10004-001-006 (to YW), and GFG is a leading principle investigator of the NSFC Innovative Research Group Grant No. 81321063. The funders had no role in study design, data collection and analysis, decision to publish, or preparation of the manuscript.

**Competing Interests:** The authors have declared that no competing interests exist.

RNA virus and a double-stranded segmented RNA virus, providing insights into the fundamental mechanisms of viral evolution.

## Author Summary

Recombination is commonly reported in coronaviruses, and is an important mechanism by which these viruses generate genetic diversity. To date, however, most such recombination events involve homologous sequences among related viruses. We discovered a novel bat coronavirus that possesses a divergent but functional p10 gene that likely originated from, or shared the ancestry with, an ancestral non-enveloped orthoreovirus, thereby representing the outcome of heterologous recombination. We report herein a fusion-associated small transmembrane (FAST) protein encoded in an enveloped virus that arose through a putative inter-family recombination between a single-stranded, positive-sense RNA virus and a double-stranded segmented RNA virus. These findings shed important new light on the mechanisms of viral evolution and particularly the importance and scope of heterologous recombination.

## Introduction

Coronaviruses are large, enveloped viruses with single-stranded, positive-sense, non-segmented RNA genomes [1]. Based on the current nomenclature of the International Committee of Taxonomy of Viruses (ICTV), coronaviruses of the family *Coronaviridae* are now classified into four genera: *alpha*-, *beta*-, *gamma*- and *deltacoronavirus* [2, 3]. Betacoronaviruses can be further subdivided into four phylogenetic groups [2].

Coronaviruses employ a unique mechanism of viral genome replication and RNA synthesis, resulting in high frequencies of both mutation and recombination [4]. Recombination appears to be particularly important in coronavirus evolution [5], with a number of hotspots interspersed throughout the viral genome [6]. Recombination events at 3'-end of the genome might impact the replication ability of coronaviruses since there are a number of regulatory sequences and accessory genes in this region [5].

As coronaviruses were previously known to cause only mild respiratory illnesses in humans they were not a major concern of the public health community. However, the emergence of severe acute respiratory syndrome coronavirus (SARS-CoV) [7–9] and its high infectivity and fatality generated considerable interest in the biodiversity, genomics, evolution, natural hosts and potential inter-species transmission of coronaviruses [10]. To date, at least 90 types of coronavirus have been isolated or genome-identified from humans and a wide variety of animals, including domestic animals, wild birds and bats. Bats are particularly notable in this respect because they are known to harbor a diverse range of pathogens, and are known to be the reservoir hosts of both human coronavirus 229E [11] and SARS-CoV [12], and are closely related to MERS-CoV [13, 14]. As a consequence bats have been prioritized for the surveillance of emerging zoonotic diseases [15–17].

In the present study we report a novel coronavirus discovered from bat samples in China that has been tentatively named Rousettus bat coronavirus GCCDC1 (Ro-BatCoV GCCDC1). Multiple lines of evidence indicate that Ro-BatCoV GCCDC1 may have arisen from a recombination event between an ancestral coronavirus and a fusogenic orthoreovirus.

## Results

### A novel coronavirus with a putative recombinant reovirus gene

A total of 118 rectal swab samples from *Rousettus leschenaulti* bats sampled in Yunnan province China were screened for the presence of coronavirus RNA. Of these, 47 (40%) samples were found to be coronavirus positive. The PCR products were sequenced and BLAST searches revealed the sequences to be authentic coronavirus genes, with the strongest similarity to *Rousettus* bat coronavirus HKU9 (Ro-BatCoV HKU9) [18], a member of the genus *betacoronavirus* (group D). However, our attempts to isolate the virus from samples using a number of cell lines, including Vero E6, BHK-21, MDCK, A549, HEp-2, CaCo-2 and a bat cell line from *Myotis* kidney, were unsuccessful. The cell lines were inoculated with positive samples and three blind passages were performed for each sample. No cytopathic effect was observed in any passage, and there was an absence of viral replication from the culture supernatant and cell pellet of each passage.

The viral genomic sequences present in two coronavirus positive samples (numbers 346 and 356) were determined with next-generation sequencing (NGS). Analysis using a partial (816-bp fragment) sequence of the RNA-dependent RNA polymerase (RdRp) gene indicated that the newly identified virus was likely to be a novel coronavirus according to previously proposed criteria [19]. Therefore, this virus was tentatively designated as *Rousettus* bat coronavirus GCCDC1 (Ro-BatCoV GCCDC1). Gaps within the genome of Ro-BatCoV GCCDC1 were closed, and the complete genome sequence confirmed, using Sanger sequencing. Finally, the 5'- and 3'-ends of Ro-BatCoV GCCDC1 genome were obtained using 5' and 3' RACE (Fig 1).

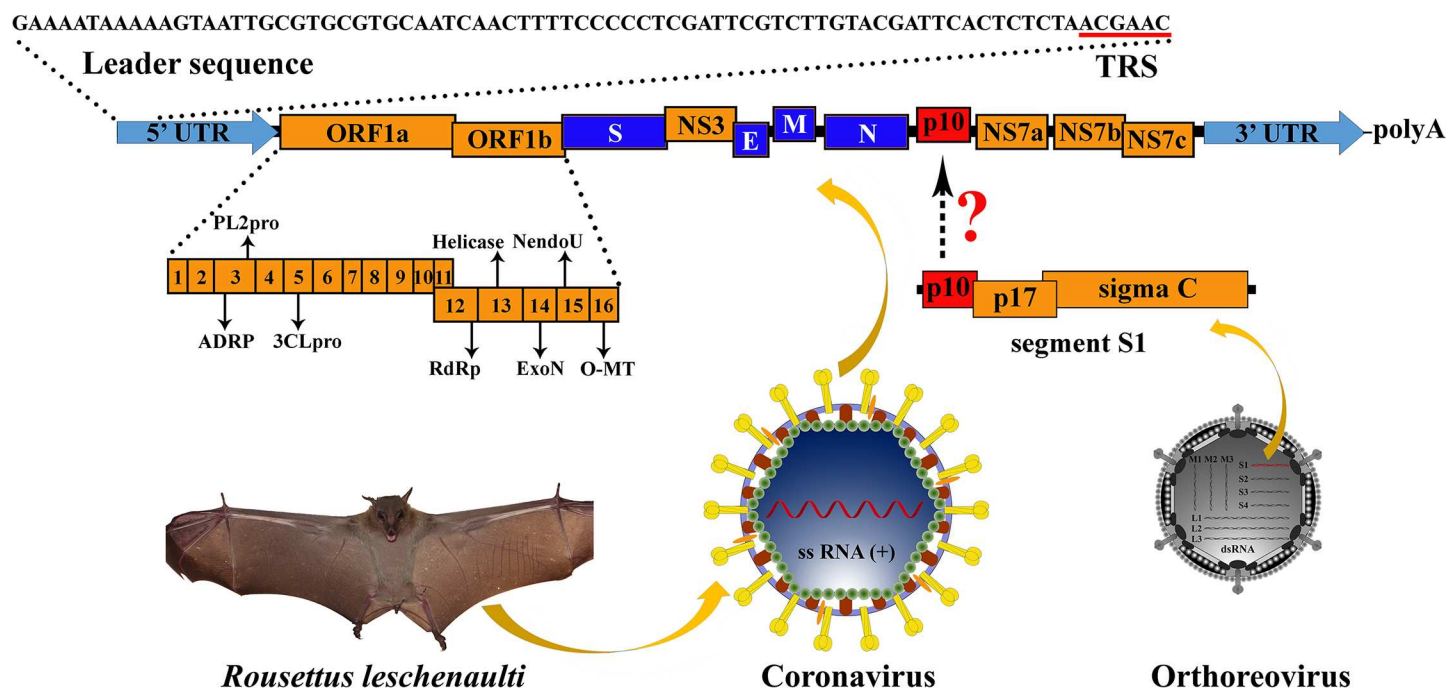


**Fig 1. Genome organization and phylogenetic history of Ro-BatCoV GCCDC1.** Genome organization of Ro-BatCoV GCCDC1. Nonstructural genes and putative mature nonstructural proteins, structural genes, and 5'- and 3'-UTR are illustrated with yellow, dark blue and light blue colors, respectively. The remarkable p10 gene is shown in red. The potential origin of the p10 gene is indicated by a dotted arrow and a question mark. The leader sequence and leader transcription regulatory sequence (TRS) are directly shown with nucleobases. The bat, *Rousettus leschenaulti*, is used to show the host species that Ro-BatCoV GCCDC1 was discovered. The schematic virion of coronavirus is used to show the virus that identified in the present study. The schematic virion of orthoreovirus and the segment S1 of the genome that it contains are used to demonstrate the possible origin of the p10 gene.

doi:10.1371/journal.ppat.1005883.g001

Excluding the polyadenylated tail at the 3'-terminus, the genome of Ro-BatCoV GCCDC1 was 30,129 nt in length with a G/C content of 45.4%. Comparative genomic sequence analysis indicated that Ro-BatCoV GCCDC1 was most closely related to Ro-BatCoV HKU9 strains [18] with 66.6% - 67.4% nucleotide identities. Similarly, Ro-BatCoV GCCDC1 displayed equivalent genomic characteristics to Ro-BatCoV HKU9 except for an inserted gene at 3' end (discussed in detail in the next section). The major open reading frames (ORFs) had the identical order, namely 5'- replicase ORF1ab—spike (S)—NS3—envelope (E)—membrane (M)—nucleocapsid (N) followed by the accessory genes encoding nonstructural proteins (NSPs) (Fig 1 and Table 1), although the N gene was truncated. Amino acid sequence analyses showed that the ORF1ab, S, NS3, E, M and N proteins of Ro-BatCoV GCCDC1 shared higher identities with Ro-BatCoV HKU9 strains than those of other betacoronaviruses (Table 1). Also of note was that the 3'-end of Ro-BatCoV GCCDC1 genome, just downstream of N gene, possessed a much more complicated structure than those of other members in the genus. Clearly, there were four NSP-encoding ORFs. According to the convention, the second-to-fourth ORFs were temporarily named NS7a, NS7b and NS7c, respectively, since they shared 29% - 53% amino acid identities with the accessory genes of Ro-BatCoV HKU9 strains and other related bat coronaviruses (S1 Table). Perhaps the most striking feature of Ro-BatCoV GCCDC1 genome was the presence of a small intact ORF with 276 bases embedded between the N and NS7a genes. Although this ORF that had no homology to any known coronavirus, the encoded protein exhibited 30% - 54.9% amino acid identity with the p10 protein encoded by the first ORF of segment S1 of avian and bat fusogenic orthoreoviruses [20], which are double-stranded segmented RNA viruses belonging to the family *Reoviridae*. Therefore, this ORF was provisionally marked as p10 according to the molar weight of protein that it encodes (Fig 1).

The putative leader and body transcription regulatory sequences (TRSs) of Ro-BatCoV GCCDC1, and their genomic localizations, were predicted in accordance with consensus core sequences of the TRSs of betacoronaviruses (Table 1). The TRS core sequence, 5'-ACGAAC-3', was consistent with those of SARS-CoV, Ro-BatCoV HKU9 and other betacoronaviruses. From the location of leader TRS, the leader sequence of the genome was then identified, which spanned genome positions 1 (G) to 78 (C) (Fig 1 and Table 1). Notably, in the putative TRS of the p10 gene, there was one nucleobase difference with the consensus core sequence (Table 1).

The putative mature nonstructural proteins (NSPs) in the ORF1ab encoding the replicase were calculated based on the cleavage and recognition pattern of the 3C-like proteinase (3CLpro) and papain-like proteinase (PLpro). Comprehensive information on the size and genomic locations of nsp1 to nsp16 and the putative cleavage sites of proteinases is presented in Table 2. Previous studies indicated that the P1 position of 3CLpro specific cleavage site is exclusively occupied by a glutamine (Q) residue [22, 23]. However, nucleobase 12642 in the Ro-BatCoV GCCDC1 genome was a T nucleotide, thereby changing glutamine (Q) to histidine (H). More interestingly, there were no glutamine codons in the sequence (from -273 to +192) around this site, as also observed in the corresponding site in the genomes of Ro-BatCoV HKU9. Therefore, the LH|AG region may represent a potential alternative cleavage site of 3CLpro to cleave between NSP9 and NSP10. A similar phenomenon may occur at the cleavage site between NSP10 and NSP12 of Ro-BatCoV GCCDC1, where the CAG codon has mutated to CAC causing the conversion of Q to H in amino acid sequence (Table 2).

Following the criteria for coronavirus species demarcation defined by the ICTV [1, 13], seven conserved replicase domains of Ro-BatCoV GCCDC1 were selected for analysis (Table 3). The amino acid identities of seven concatenated domains in Ro-BatCoV GCCDC1 revealed that they shared 84.4% - 84.8% identity with those of Ro-BatCoV HKU9, which was below the 90% threshold used for species demarcation (Table 3). Hence, these data suggest that



**Table 1. Coding potential, transcription regulatory sequences and sequence comparisons of Ro-BatCoV GCCDC1 with Ro-BatCoV HKU9 strains, SARS-CoV, BatCoV HKU3 stains, MERS-CoV, BatCoV HKU4 strains and BatCoV HKU5 strains.**

| ORFs                    | Nucleotide positions (start to end) | Predicted size (aa) of protein | Pairwise amino acid identity (%) <sup>a</sup> Ro-BatCoV GCCDC1 vs |                       |                    |                       |                    |                    | Leader TRS region and intergenic TRS <sup>b</sup> | Distance (nt) from TRS to ATG |
|-------------------------|-------------------------------------|--------------------------------|---|-----------------------|--------------------|-----------------------|--------------------|--------------------|---|-------------------------------|
|                         |                                     |                                | HKU9s <sup>c</sup>  | SARS-CoV <sup>d</sup> | HKU3s <sup>e</sup> | MERS-CoV <sup>f</sup> | HKU4s <sup>g</sup> | HKU5s <sup>h</sup> |   |                               |
| <b>ORF 1ab</b>          | 235–21155                           | 6973                           | 74.6–75.4   | 47.1                  | 47.3–47.4          | 46.3                  | 45.7–45.8          | 46.1–46.2          | TCTA <b><u>ACGA</u>ACTTAA</b>                     | 156                           |
| <b>Spike</b>            | 21121–24993                         | 1290                           | 58.8–66.4   | 32.1                  | 31.3–31.4          | 27.9                  | 28.4–28.6          | 27.7–27.8          | CTGA <b><u>ACGA</u>ACTAGT</b>                     | 42                            |
| <b>NS3<sup>i</sup></b>  | 24990–25676                         | 228                            | 48.9–50.7   | NA                    | NA                 | NA                    | NA                 | NA                 | GAAA <b><u>ACGA</u>ACGGCA</b>                     | 3                             |
| <b>E</b>                | 25676–25906                         | 76                             | 61.8–69.7   | 32.9                  | 32.9               | 23.7                  | 26.3               | 26.3               | GATGT <b><u>TCGA</u>ACTGTG</b>                    | 4                             |
| <b>M</b>                | 25914–26579                         | 221                            | 75.6–80.5   | 43.2                  | 42.3–42.7          | 41.1                  | 41.1               | 43.6               | TCTA <b><u>ACGA</u>ACAGGA</b>                     | 27                            |
| <b>N</b>                | 26627–27958                         | 443                            | 68.0–71.7   | 39.1                  | 39.5–40.0          | 41.7                  | 41.4–41.7          | 38.4–38.7          | GGAA <b><u>ACGA</u>ACCTAT</b>                     | 5                             |
| <b>p10<sup>j</sup></b>  | 27994–29269                         | 91                             | NA  | NA                    | NA                 | NA                    | NA                 | NA                 | AATG <b><u>ACAAA</u>CCCAA</b>                     | 97                            |
| <b>NS7a<sup>k</sup></b> | 28287–28850                         | 187                            | 40.0  | NA                    | NA                 | NA                    | NA                 | NA                 | TCTA <b><u>ACGA</u>ACTCAT</b>                     | 5                             |
| <b>NS7b<sup>l</sup></b> | 28863–29444                         | 193                            | 32.0–42.0   | NA                    | NA                 | NA                    | NA                 | NA                 | TCTA <b><u>ACGA</u>ACTATG</b>                     | 1                             |
| <b>NS7c<sup>m</sup></b> | 29444–29893                         | 149                            | 30.0–53.0   | NA                    | NA                 | NA                    | NA                 | NA                 | GTAG <b><u>ACGAA</u>CTTTG</b>                     | 4                             |

**a:** Calculated with MEGA6 [21] using a pairwise deletion option [13].

**b:** Underlined and bold type indicates the conserved nucleotide in the TRS core sequence.

**c:** GenBank accession numbers of the viruses used in this analysis: NC\_009021, EF065514, EF065515, EF065516, HM211098, HM211099, HM211100, HM211101.

**d:** GenBank accession numbers of the viruses used in this analysis: NC\_004718.

**e:** GenBank accession numbers of the viruses used in this analysis: DQ022305, DQ084199, DQ084200, GQ153539, GQ153540, GQ153541, GQ153542, GQ153543, GQ153544, GQ153545, GQ153546, GQ153547, GQ153548.

**f:** GenBank accession numbers of the viruses used in this analysis: NC\_019843.

**g:** GenBank accession numbers of the viruses used in this analysis: NC\_009019, EF065506, EF065507, EF065508.

**h:** GenBank accession numbers of the viruses used in this analysis: NC\_009020, EF065510, EF065511, EF065512.

**i:** In the genomes of Ro-BatCoV GCCDC1, Ro-BatCoV HKU9 strains, SARS-CoV, BatCoV HKU3 strains, MERS-CoV, BatCoV HKU4 strains and BatCoV HKU5 strains, the organization of the region between the spike and E genes is divergent; there is no comparability of ORFs in this region.

**j:** As the p10 gene is specific to Ro-BatCoV GCCDC1, there are no homologous genes in the genomes of Ro-BatCoV HKU9, SARS-CoV, BatCoV HKU3, MERS-CoV, BatCoV HKU4 or BatCoV HKU5.

**k:** The NS7a protein of Ro-BatCoV GCCDC1 shares 40% amino acid identity (87% coverage) with the NS7a protein of Bat coronavirus HKU9-1; There is no comparability with any ORF of other coronaviruses.

**l:** The NS7b protein of Ro-BatCoV GCCDC1 shares 32% - 42% amino acid identity (88% - 91% coverage) with the NS7a proteins of Bat coronavirus HKU9-3, HKU9-4, HKU9-10-1 and HKU9-10-2.

**m:** The NS7c protein of Ro-BatCoV GCCDC1 shares 30% - 53% amino acid identity (90% - 99% coverage) with the NS7b protein of Bat coronavirus HKU9-1, HKU9-2, HKU9-3, HKU9-4, HKU9-10-1 and HKU9-10-2.

doi:10.1371/journal.ppat.1005883.t001

the newly identified Ro-BatCoV GCCDC1 represents a novel coronavirus species in the genus *betacoronavirus*.

To determine the evolutionary position of Ro-BatCoV GCCDC1, the RdRp, S, N and p10 proteins were subjected to phylogenetic analyses. Phylogenetic trees of the RdRp, S and N proteins illustrated that Ro-BatCoV GCCDC1, Eidolon bat coronavirus/Kenya/KY24/2006 (Ei-BatCoV Kenya), Rousettus bat coronavirus/Kenya/KY06/2006 (Ro-BatCoV Kenya) and Ro-BatCoV HKU9 strains all belong to group D of the genus *betacoronavirus* (Fig 2). Within this

**Table 2. Prediction of the putative pp1a/pp1ab cleavage sites of Ro-BatCoV GCCDC1 based on comparison with prototype coronaviruses<sup>a</sup>.**

| NSP   | amino acids positions in ORF1a/ORF1b | Predicted size (aa) of protein | C-end putative cleavage site | Putative functional domain(s) <sup>b</sup>  |
|-------|--------------------------------------|--------------------------------|------------------------------|---|
| NSP1  | M <sup>1</sup> -G <sup>174</sup>     | 174                            | RG GN                        | Unknown                                     |
| NSP2  | G <sup>175</sup> -G <sup>772</sup>   | 598                            | GG GK                        | Unknown                                     |
| NSP3  | G <sup>773</sup> -G <sup>2653</sup>  | 1881                           | VG GN                        | ADRP, PL2 pro                               |
| NSP4  | G <sup>2654</sup> -Q <sup>3147</sup> | 494                            | LQ AG                        | Hydrophobic domain                          |
| NSP5  | A <sup>3148</sup> -Q <sup>3453</sup> | 306                            | LQ SR                        | 3CL pro                                     |
| NSP6  | S <sup>3454</sup> -Q <sup>3741</sup> | 288                            | IQ SN                        | Hydrophobic domain                          |
| NSP7  | S <sup>3742</sup> -Q <sup>3824</sup> | 83                             | LQ AV                        | Unknown                                     |
| NSP8  | A <sup>3825</sup> -Q <sup>4024</sup> | 200                            | LQ NN                        | Primase                                     |
| NSP9  | N <sup>4025</sup> -H <sup>4136</sup> | 112                            | LH AG                        | Unknown                                     |
| NSP10 | A <sup>4137</sup> -H <sup>4275</sup> | 139                            | LH AN                        | Unknown                                     |
| NSP11 | A <sup>4276</sup> -S <sup>4289</sup> | 14                             |                              | Unknown (short peptide at the end of ORF1a) |
| NSP12 | A <sup>4276</sup> -Q <sup>5207</sup> | 932                            | LQ SV                        | RdRp  |
| NSP13 | S <sup>5207</sup> -Q <sup>5808</sup> | 601                            | TQ SA                        | HEL, NTPase                                 |
| NSP14 | S <sup>5809</sup> -Q <sup>6338</sup> | 530                            | LQ SL                        | ExoN, NMT                                   |
| NSP15 | S <sup>6339</sup> -Q <sup>6680</sup> | 342                            | LQ SK                        | NendoU                                      |
| NSP16 | S <sup>6681</sup> -V <sup>6973</sup> | 293                            |                              | O-MT  |

a: GenBank accession numbers of the viruses used in this analysis: SARS-CoV, NC\_004718; HCoV HKU1, NC\_006577; IBV, NC\_001451; TCoV, NC\_010800; BCov, NC\_003045; MHV, NC\_001846; and PEDV, NC\_003436.

b: ADRP, ADP-ribose 1-phosphatase; PL2pro, papain-like protease 2; 3CL pro, coronavirus nsp5 protease; HEL, helicase; NTPase, nucleoside triphosphatase; ExoN, exoribonuclease; NMT, N7 methyltransferase; NendoU, endoribonuclease; OMT, 2'-O-methyltransferase.

doi:10.1371/journal.ppat.1005883.t002

cluster the two Ro-BatCoV GCCDC1 strains (346 and 356) formed a distinct lineage that was a sister-group to Ro-BatCoV Kenya and the Ro-BatCoV HKU9 strains (maximum bootstrap

**Table 3. Comparison of amino acid identities of seven conserved replicase domains of Ro-BatCoV GCCDC1 for species classification.**

| Coronavirus CDDC1 strain 356 | amino acid identity (%) <sup>a</sup> |                       |                    |                       |                    |                    |
|------------------------------|--------------------------------------|-----------------------|--------------------|-----------------------|--------------------|--------------------|
|                              | HKU9s <sup>b</sup>                   | SARS-CoV <sup>c</sup> | HKU3s <sup>d</sup> | MERS-CoV <sup>e</sup> | HKU4s <sup>f</sup> | HKU5s <sup>g</sup> |
| ADRP                         | 65.8–68.3                            | 48.8                  | 49.4–50.0          | 45.0                  | 42.5–43.1          | 39.4               |
| NSP5 (3CL pro)               | 83.3–84.3                            | 52.3                  | 52.0–52.3          | 49.2                  | 49.8               | 49.5–49.8          |
| NSP12 (RdRp)                 | 89.8–90.3                            | 72.3                  | 72.3–72.4          | 69.7                  | 70.1–70.2          | 70.5–70.6          |
| NSP13 (Hel, NTPase)          | 90.8–91.5                            | 73.7                  | 73.7–74.0          | 72.7                  | 73.1               | 72.9–73.1          |
| NSP14 (ExoN, NMT)            | 82.1–82.8                            | 61.4                  | 61.8–62.1          | 61.1                  | 60.1               | 60.7               |
| NSP15 (NendoU)               | 70.9–73.3                            | 49.7                  | 49.4–49.7          | 46.6                  | 46.0               | 47.5–47.8          |
| NSP16 (OMT)                  | 80.1–84.2                            | 63.8                  | 63.1–63.5          | 61.8                  | 62.1               | 62.5               |
| Concatenated domains         | 84.4–84.8                            | 64.4                  | 64.4–64.6          | 62.4                  | 62.3–62.4          | 62.5–62.6          |

a: Calculated with MEGA6 [21] using a pairwise deletion option [13].

b: GenBank accession numbers: NC\_009021, EF065514, EF065515, EF065516, HM211098, HM211099, HM211100, HM211101.

c: GenBank accession number: NC\_004718.

d: GenBank accession numbers: DQ022305, DQ084199, DQ084200, GQ153539, GQ153540, GQ153541, GQ153542, GQ153543, GQ153544, GQ153545, GQ153546, GQ153547, GQ153548.

e: GenBank accession numbers: NC\_019843.

f: GenBank accession numbers: NC\_009019, EF065506, EF065507, EF065508.

g: GenBank accession numbers: NC\_009020, EF065510, EF065511, EF065512.

doi:10.1371/journal.ppat.1005883.t003

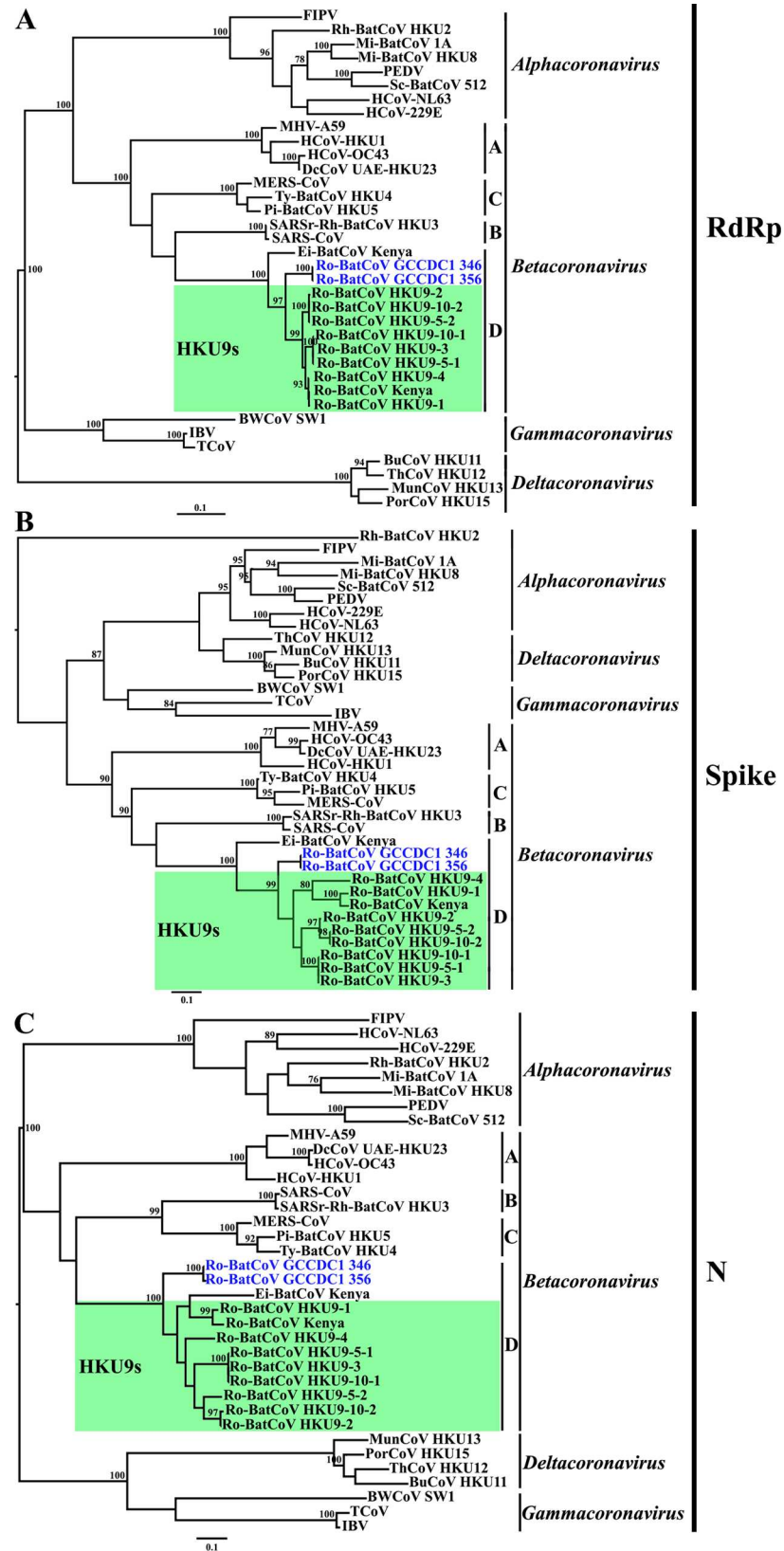




**Fig 2. Phylogenetic analyses of representative coronaviruses, including Ro-BatCoV GCCDC1.** All trees (A: RdRp; B: S and C: N) were inferred using the maximum likelihood method available in PhyML. Bootstrap values are shown at relevant nodes. The GenBank accession numbers used in this analysis are listed in [S2 Table](#).

doi:10.1371/journal.ppat.1005883.g002

value of 100%). However, a strikingly different phylogenetic pattern was observed in the distinctive p10 protein ([Fig 3](#)), in which the Ro-BatCoV GCCDC1 sequences were clearly related to bat (Pteropine) originated orthoreoviruses. Although the branch leading to the Ro-BatCoV GCCDC1 sequences is long, these viruses are clearly more closely related to the bat-origin than avian-origin orthoreoviruses ([Fig 3](#)), matching the host species from which Ro-BatCoV GCCDC1 was isolated.

## Evidence for heterologous recombination of a reovirus p10 gene recombination into Ro-BatCoV GCCDC1

To exclude the false amplification of DNA polymerase or the inaccurate assembly of NGS data, the NGS data was analyzed further. Read mapping determined that there were a set of reads that covered the upstream junction site (i.e. the recombination break-point) between N and p10 genes, and a downstream junction site between the p10 and NS7a genes ([S1 Fig](#) with data in [S1 File](#)). In addition, the integrity and continuity of context sequence surrounding the p10 gene were confirmed with specific primers. Agarose gel electrophoresis showed that the PCR products were intact fragments of the expected length. The amplicons were cloned for sequencing. As shown in [Fig 4A](#), the sequence obtained covers, without interruption, the partial N gene, the whole p10 gene and partial NS7a gene (data in the [S2 File](#)). Hence, there is clear evidence that the recombination event that placed the reovirus p10 gene in the Ro-BatCoV GCCDC1 genome was genuine.

Sequencing information confirmed that the TRS of p10 gene is located within the encoding sequence of N gene with the core sequence of 5'-ACAAAC-3', which exhibited a single nucleobase difference to the consensus core sequence (5'-ACGAAC-3') ([Fig 4B](#)). We also observed a 97 nucleobase sequence between the TRS and the p10 initiation codon ([Fig 4B](#)), which was much longer than the intervening sequences of other genes with the exception for that between the leader TRS and ORF1ab ([Table 1](#)). As shown in [Fig 4B](#) and [S2 Fig](#), sequence comparisons also revealed that the location of TRS in the p10 gene could be discriminated from those of other genes, which are adjacent and downstream to the N gene of Group D *Betacoronavirus*. Notably, the ORF of the Ro-BatCoV GCCDC1 N gene was disrupted by the insertion of the "exotic" p10 gene, causing the truncation of eight amino acids at the 3'-terminus and a two amino acid deletion ([Fig 5](#)).

## Subgenomic structures of Ro-BatCoV GCCDC1

According to the information provided above, the relative locations of the putative leader and body TRS(s) were identified in the genome of Ro-batCoV GCCDC1 ([Fig 6A](#)). Based on the TRSs and transcription mechanism of coronavirus, nine potential subgenomic mRNAs of Ro-BatCoV GCCDC1, including S, NS3, E, M, N, p10, NS7a, NS7b and NS7c, were depicted ([Fig 6B](#)). In addition to an identical 5' leader sequence, each lower subgenomic mRNA shared the same 3'-end structure with the upper one to comprise a 3' co-terminal nested set with the genome.

The presence of subgenomic mRNAs is strong evidence of coronavirus replication in the infected cells. To determine if the bat, which sample was collected from, was likely the natural host of Ro-BatCoV GCCDC1, subgenomic mRNAs in the sample were probed with a

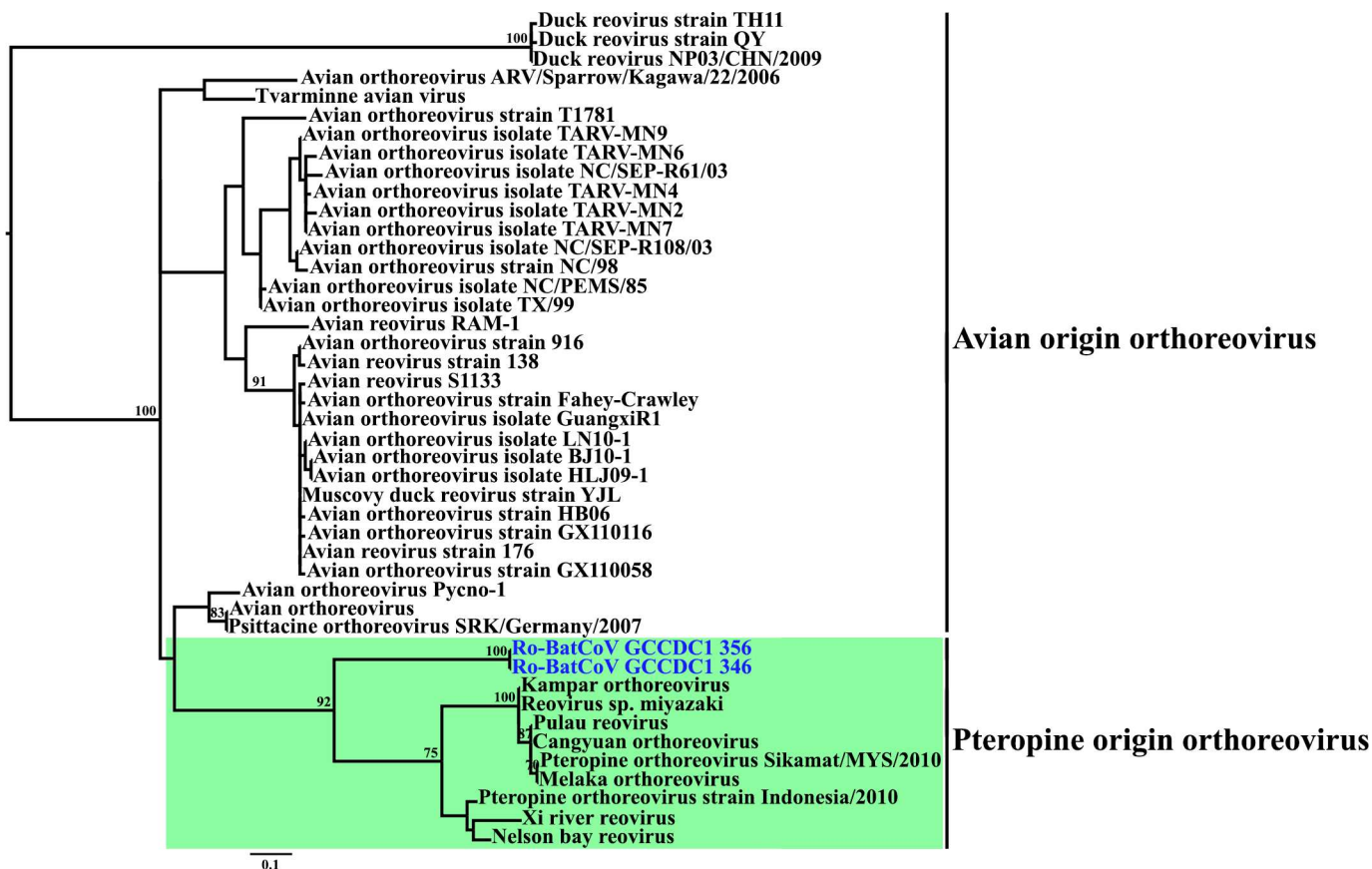


**Fig 3. Phylogenetic analyses of p10 from representative reoviruses and Ro-BatCoV GCCDC1.** The tree was inferred using the maximum likelihood method available in PhyML. Bootstrap values are shown at relevant nodes. The GenBank accession numbers used in this analysis are listed in S3 Table.

doi:10.1371/journal.ppat.1005883.g003

comprehensive set of primers. The PCR products were confirmed on an agarose gel. As displayed in Fig 6C, the lowest band marked with a red arrow on each lane was the specific amplicon from each subgenomic mRNA as demonstrated in Fig 6B. However, additional amplified bands were also compatible with this inference. As shown as an example on the lane of the E gene, the upper band indicates that subgenomic mRNA NS3 was simultaneously amplified in this reaction. On each lane the lowest band was cloned for sequencing, while other bands were purified and sequenced directly. Since the specific amplicon of the subgenomic mRNA NS7c failed to be cloned into the vectors, the PCR product was used as template for a second round of nested PCR. The product was then confirmed as shown in the lane of NS7c-2 in Fig 6C, and the band was cloned for sequencing. The results (Fig 6D and S3 Fig) indicated that the core sequence of the leader and body TRS of each gene, the leader-body fusion sites, and the mode of generation of subgenomic mRNAs were consistent with the prediction and demonstration in Fig 6B, especially the p10 gene and its subgenomic mRNA. Therefore, the existence of subgenomic mRNA in the samples further proved that the p10 gene was an intact authentic gene in the genome of Ro-BatCoV GCCDC1.

### The p10 gene of Ro-BatCoV GCCDC1 is functional

Despite the orthoreovirus origin of p10, this protein exhibited 8 amino acid differences (including a 2 amino acid deletion) among the 28 “absolutely conserved” amino acids described

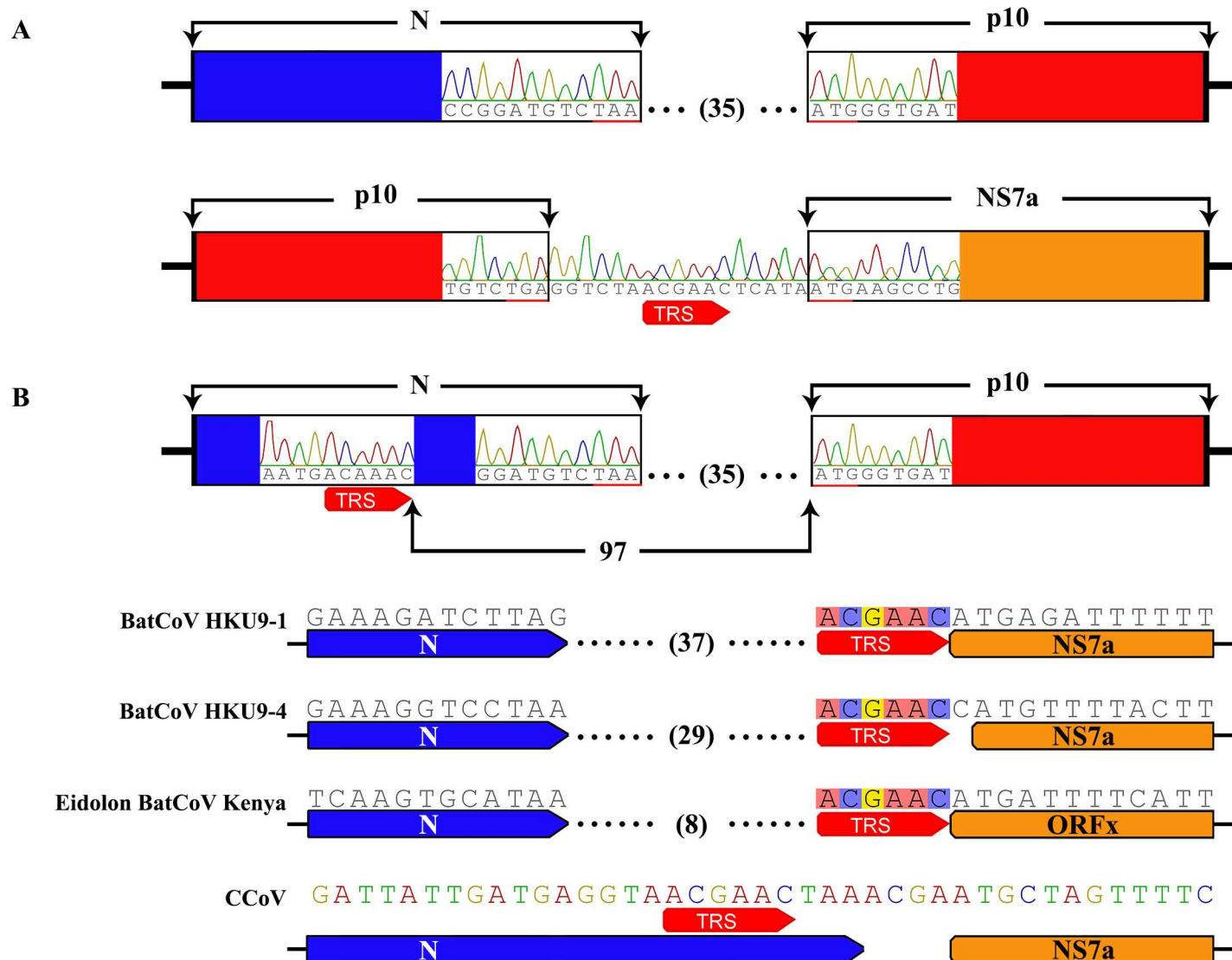


**Fig 4. Identification of the recombinant p10 gene and its TRS.** (A) Confirmation of the “exotic” p10 gene. The sequences that cover the upstream junction site between the N and p10 genes, and downstream junction site between the p10 and NS7a genes, are illustrated with sequencing patterns. The length of the intergenic sequence between the N and p10 genes is indicated with a number. The TRS preceding the NS7a gene in the intergenic sequence is marked with red arrow. (B) Identification of the TRS of the p10 gene. The TRS of the p10 gene in the N gene is illustrated with a sequencing pattern. The distance from the TRS to the AUG codon of p10 gene is indicated with a number. The length of the intergenic sequence between the N gene and genes just downstream of N gene are indicated with numbers. The TRSs of genes just downstream of N gene are marked with red arrows.

doi:10.1371/journal.ppat.1005883.g004

previously (Fig 7). Hence, it is necessary to investigate whether the p10 gene of Ro-BatCoV GCCDC1 could play the same role as its reovirus homologs. For this purpose, the p10 gene of Ro-BatCoV GCCDC1 was transiently expressed in BHK-21 cells as well as the p10 gene of Pulau virus, which was used as a positive control. Wright-Giemsa and immunofluorescence staining showed that both genes had the same function to induce the formation of cell syncytia (Fig 8A and 8B and S4A Fig). Thus, the alteration of certain conserved amino acids did not impair the syncytiogenesis of p10 gene of Ro-BatCoV GCCDC1.

The p10 subgenomic mRNA identified in the samples confirmed that the p10 gene could be transcribed from the genome of Ro-BatCoV GCCDC1. However, due to the failure of virus isolation (despite a great effort), there is no effective way to judge whether the p10 gene could be

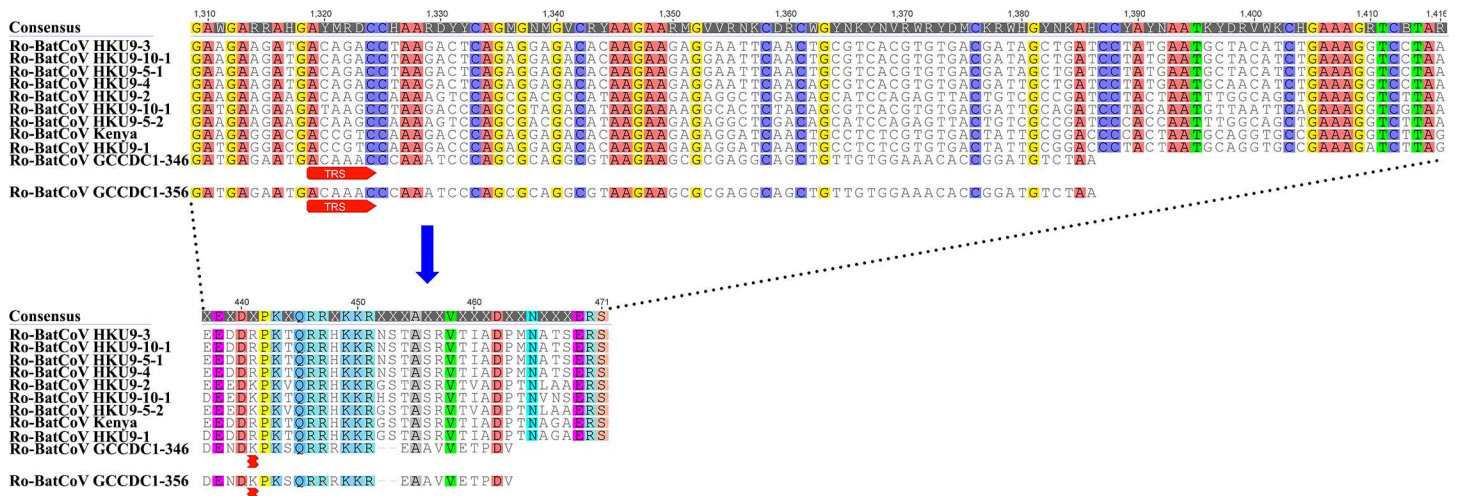


**Fig 5. Comparison of the 3'-terminus of the N gene of Ro-BatCoV GCCDC1 with those of Ro-BatCoV HKU9 strains and Ro-BatCoV Kenya.** Alignment of nucleotide and amino acid sequence of the 3'-terminus of the N gene among Ro-BatCoV GCCDC1, Ro-BatCoV HKU9 strains and Ro-BatCoV Kenya. The eight amino acid truncation and two-amino-acid deletion at the 3'-terminus of N protein of the Ro-BatCoV GCCDC1 are illustrated.

doi:10.1371/journal.ppat.1005883.g005

expressed during the virus replication cycle. Therefore, an artificial plasmid was constructed containing the transcribed p10 subgenomic mRNA, which confirmed the functional expression of p10 (Fig 8C). When the plasmid was transfected into BHK-21 cells, once again, cell syncytia were observed with Wright-Giemsa and immunofluorescence staining (Fig 8D and S4B Fig). Thus, this indirect evidence suggests that the p10 gene functions during the replication cycle of Ro-BatCoV GCCDC1.

Immunofluorescence staining also showed that polyclonal antibodies of Ro-BatCoV GCCDC1 p10 protein reacted with the p10 protein of Pulau virus (Fig 8B and Fig 8D). In addition, the cross-reactivity further proved that the p10 gene of Ro-BatCoV GCCDC1 might have the same origin as those of fusogenic orthoreoviruses.

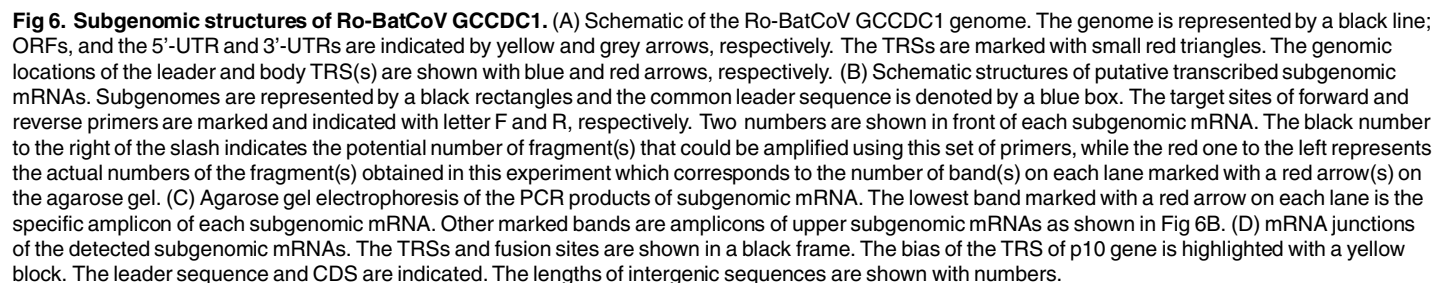
As the p10 protein of Ro-BatCoV GCCDC1 is the first report of FAST protein in an enveloped virus, the conserved amino acids of the p10 protein of Ro-BatCoV GCCDC1 were mutated to determine whether they play a vital role in cell-to-cell fusion and syncytium formation as those sites in the p10 protein of reoviruses (S5A Fig) [24, 25]. Notably, no cell syncytia were observed for all mutant constructs of p10 which had substitutions in the previously defined key sites in the p10 protein of reoviruses (S5B Fig). This indicates that the functionality of p10 in Ro-BatCoV GCCDC1 also depends on traditional conserved domains relevant for the function of the FAST protein [24, 25].

To confirm the expression of p10 by the Ro-BatCoV GCCDC1 virus, we performed Western blotting (WB) to detect the presence of p10 protein in the bat feces and concentrated rectal swab specimens. The results revealed the expression of p10 by Ro-BatCoV GCCDC1 itself (S6 Fig).

## Discussion

We have identified a novel coronavirus, Ro-BatCoV GCCDC1, from *Rousettus leschenaulti*, that belongs to group D of the genus *betacoronavirus* and which is related to Ro-BatCoV HKU9 [18]. According to the criteria defined by ICTV [1], Ro-BatCoV GCCDC1 is sufficiently divergent to represent a novel bat coronavirus. More striking was that Ro-BatCoV GCCDC1





contains a p10 protein located at the 3'-end of the genome that appears to have captured from a bat-origin orthoreovirus by heterologous recombination.

## Avian Reoviruses

Duck reovirus strain 091  
Duck reovirus strain QY  
Duck reovirus strain TH11  
Avian orthoreovirus strain HB06  
Avian orthoreovirus strain GX110116  
Avian orthoreovirus strain GX110058  
Avian orthoreovirus isolate GuangxiR1  
Avian orthoreovirus strain 916  
Avian orthoreovirus isolate TARV-MN4  
Avian orthoreovirus isolate TARV-MN7  
Avian orthoreovirus isolate TARV-MN6  
Avian orthoreovirus isolate TARV-MN2  
Avian orthoreovirus isolate TARV-MN3  
Avian orthoreovirus strain T1781  
Avian orthoreovirus  
Avian orthoreovirus strain Pycno-1  
Tvarminne avian virus

Avian reovirus strain 176  
Avian reovirus strain S1133  
Muscovy duck reovirus strain YJL  
Avian reovirus strain 138  
RAM-1  
Avian orthoreovirus isolate NC/SEP-R108/03  
Avian orthoreovirus strain NC/98  
Avian orthoreovirus isolate NC/SEP-R61/03  
Avian orthoreovirus isolate TX/99  
Avian orthoreovirus isolate NC/PEMS/85  
Psittacine orthoreovirus SRK/Germany/2007

## Pteropine Reoviruses

Melaka orthoreovirus  
Pteropine orthoreovirus Sikamat/MYS/2010  
Pulau reovirus  
Kampar orthoreovirus  
Nelson bay reovirus  
Reovirus sp. miyazaki  
Pteropine orthoreovirus strain Indonesia/2010  
Xi river reovirus  
Cangyuan orthoreovirus  
Ro-BatCoV GCCDC1 stain 346  
Ro-BatCoV GCCDC1 stain 356

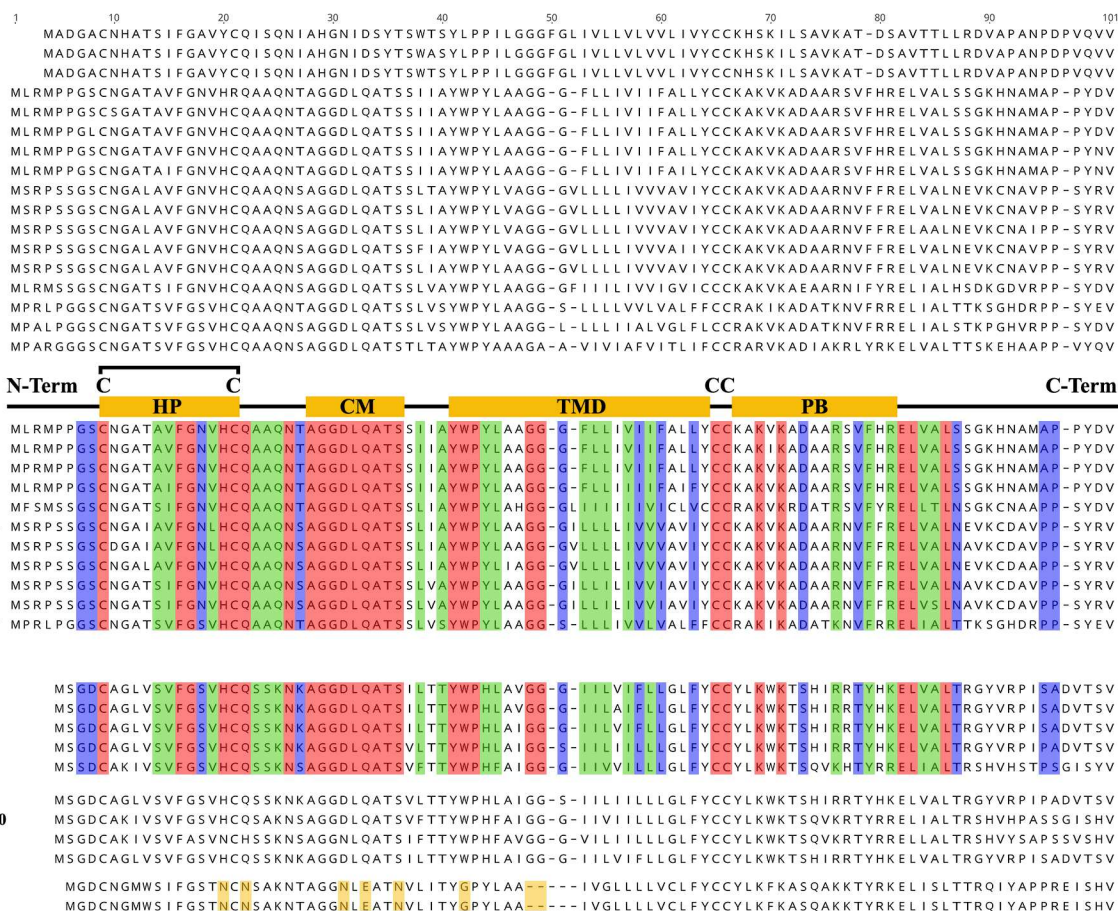


**Fig 7. Comparison of the p10 protein of Ro-BatCoV GCCDC1 with those of avian and bat origin orthoreovirus.** The absolutely, highly, moderately and non-conserved amino acids of p10 proteins as defined previously [26], are illustrated with red, blue, green and black colors, respectively. The motifs and domains in the p10 molecule are represented as previously reported [26]. Motifs present in the ectodomain (HP, hydrophobic patch; CM, conserved motif), endodomain (PB, polybasic) and the central transmembrane domain (TMD) are depicted with yellow rectangles. The four conserved cysteine residues (C) are shown. The two cysteines in the ectodomain form an intra-molecular disulfide bond. Comparison of the p10 protein of Ro-BatCoV GCCDC1 with those of avian and bat origin orthoreoviruses, the 8 different amino acids (including a 2 amino acid deletion) in the 28 absolutely conserved amino acids are symbolized with red star.

doi:10.1371/journal.ppat.1005883.g007

Homologous recombination events frequently occur during the viral RNA replication of coronaviruses, and are important for their evolution [10, 27–29]. However, it is also possible that coronaviruses are one of the few virus families that can experience heterologous recombination. For example, members of *betacoronavirus* group A possess an HE gene [30, 31] which was seemingly derived from ancestral influenza C virus, a negative-stranded RNA virus with a segmented genome [30, 31], and which would represent another case of inter-family recombination, although it has also been proposed that the HE gene might be captured from host RNA [32]. Uncommon inter-family recombination events have also been reported in chicken infectious anemia virus [33], bandicoot papillomatosis carcinomatosis virus type 1 [34], and recombinant viruses between Marek's disease virus, fowlpox virus, and various avian retroviruses [35, 36]. In the current study, sequence, phylogenetic and functional analyses demonstrated that the p10 gene of Ro-BatCoV GCCDC1 was likely derived from an ancestral orthoreovirus, although that it occupies a divergent position in the phylogeny suggests that the direct ancestor of the recombination event has yet to be sampled. Hence, these data provide clear evidence for



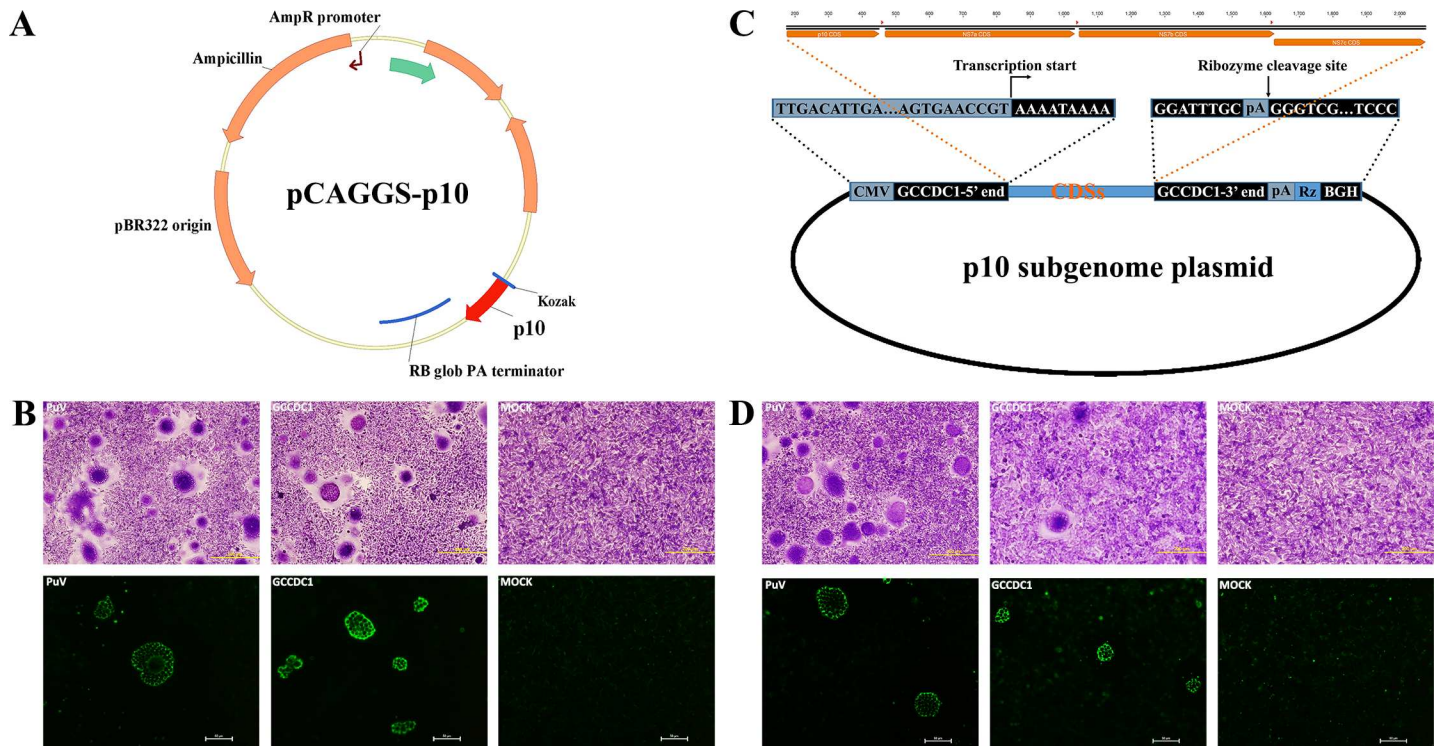


**Fig 8. Syncytium formation and functional analyses of Ro-BatCoV GCCDC1 p10 gene.** (A) The construction of transient expression plasmid of p10 gene based on a pCAGGS vector. (B) Transient expression of the p10 gene and syncytium formation. **Top:** the observation of syncytium formation with Wright-Giemsa staining on the monolayer BHK-21 cells transfected with recombinant plasmid of Pulau virus p10 gene, recombinant plasmid of Ro-BatCoV GCCDC1 p10 gene, and empty pCAGGS vector; **Bottom:** the observation of syncytium formation with indirect immunofluorescence staining on the cells treated as described above. (C) The construction of subgenomic plasmid of p10 gene. The putative subgenome of p10 was cloned into a pcDNA3.0-derived vector. (D) Transient expression of the p10 gene and syncytium formation with recombinant subgenomic p10 plasmid. **Top:** the observation of syncytium formation with Wright-Giemsa staining on the monolayer BHK-21 cells transfected with recombinant plasmid of Pulau virus p10 gene, recombinant plasmid of p10 subgenome of Ro-BatCoV GCCDC1 and empty pcDNA3.0 vector; **Bottom:** the observation of syncytium formation with indirect immunofluorescence staining on the cells treated as described above. (Wright-Giemsa staining: stained monolayers were imaged using an Olympus IX51FL+DP70 microscope under 100× magnification, scale bars = 200 μm; indirect immunofluorescence staining: stained monolayers were imaged using a Nikon DIAPHOT-TMD microscope under 200× magnification, scale bars = 50 μm).

doi:10.1371/journal.ppat.1005883.g008

a putative inter-family recombination between a single-stranded, positive-sense RNA virus and a double-stranded segmented RNA virus. The mechanisms that underpin such inter-family heterologous recombination clear merit further investigation.

The biggest difference between fusogenic and nonfusogenic orthoreoviruses is the presence/absence of a small protein encoded by the segment S1 of the genome, termed the fusion-associated small transmembrane (FAST) protein. The FAST proteins are the only known nonenveloped reovirus fusogens that can mediate cell-to-cell, but not virus-cell, membrane fusion to induce the formation of syncytia [20], and which might promote the dissemination of virus among cells [37]. Thus, the FAST proteins are the pathogenic determinants of fusogenic orthoreoviruses. To date, the FAST family comprises six members including p10 proteins encoded by avian- and bat-origin orthoreoviruses, p13, p14 and p15 encoded by broome virus, reptilian reovirus and bush viper reovirus and baboon orthoreovirus respectively, and p16 and p22 encoded by aquareoviruses. Intriguingly, a specific p10 gene was identified in Ro-BatCoV GCCDC1, so that this is the first report of a FAST protein in an enveloped virus and hence could represent the seventh member of FAST family.

Unfortunately, the isolation of Ro-BatCoV GCCDC1 failed on cell culture in the present study, so it is difficult to determine the role of p10 gene during the life cycle of Ro-BatCoV GCCDC1. However, functional analysis showed that the coronavirus p10 gene could induce syncytium formation in the transfected cells, in the same manner as orthoreoviruses, which might be beneficial for cell-to-cell virus spread. It is therefore possible that the p10 protein enhances the transmission potential of Ro-BatCoV GCCDC1. Previous studies of the potential recombination between coronavirus and influenza C virus revealed the pivotal role of the shared HE gene for the pathogenesis of *betacoronavirus* group A [38]. Interestingly, human coronavirus HKU1, OC43 and bovine coronaviruses employ the HE protein to mediate receptor-destroying enzyme activity late in the infection cycle to facilitate viral progeny release and achieve efficient virus dissemination [39].

Compared to nonfusogenic orthoreoviruses, fusogenic orthoreoviruses can cause severe pneumonia when infecting humans [40, 41], further implying that p10 is an important pathogenic determinant. Thus, the recombination of the reovirus-originated p10 into the Ro-BatCoV GCCDC1 may enable the novel virus to disseminate and replicate rapidly in the host, in turn leading to severe infections. In recent years, several coronaviruses, notably SARS-CoV and MERS-CoV, have caused severe pneumonia among humans [42, 43]. Because of the presence of human infected fusogenic orthoreoviruses such as Melaka virus (MelV) [44], there is obviously some risk that cross-family recombination events such as that described here may generate a novel coronavirus with altered pathogenicity. Our study therefore highlights the importance of investigating the mechanisms that might enable possible recombination between human coronaviruses and orthoreoviruses.

In the protein sequence of ORF1ab encoded replicase of Ro-BatCoV GCCDC1, the regular P1 position at two 3CLpro cleavage sites, NSP9/NSP10 and NSP10/NSP12, contains a Q to H mutation which may impair the proteolytic efficacy and the release of NSP9, NSP10 and NSP12. As NSP12 is a typical RNA polymerase and the core of replication-transcription complexes (RTC) and NSP10 usually serves as a molecular switch that can interact with multiple NSPs to form complexes, the replication ability of Ro-BatCoV GCCDC1 might be suppressed by the decrease of release of these vital elements. It is also interesting to note that a similar situation may be observed at the NSP13/NSP14 cleavage sites of replicase polyprotein of human coronavirus HKU1 and human coronavirus NL63. Clearly, further investigation will need to focus on the isolation of the virus, construction of infectious clones, and the virulence and replication ability of Ro-BatCoV GCCDC1 influenced by knockout of p10 gene and/or reverse mutation of cleavage sites.

Phylogenetically distinct virus species or lineages have been reported co-circulating in certain bat populations [45, 46]. Under this situation, co-infections of single host cells—the necessary requisite for recombination—are possible. By careful sequence analysis we show that the heterologous recombination event placed the p10 gene in Ro-BatCoV GCCDC1 is genuine. Previous studies showed the existence of p10-harboring orthoreoviruses in bat populations [40, 47–49], such that co-infections with bat coronaviruses and hence recombination events are clearly possible. In addition, a previous study reported that mammalian orthoreovirus, a type of nonfusogenic orthoreovirus, was isolated from a SARS-CoV patient along during the in 2003 outbreak [50]. We believe that future studies should investigate co-infections in specific bat cell lines using a coronavirus similar to Ro-BatCoV GCCDC1 or Ro-BatCoV HKU9 and the relevant orthoreoviruses, from which it will be possible to reveal more of the underlying basis of heterologous coronavirus recombination.

## Materials and Methods

### Ethics statement

The protocol in this study was approved by the Committee on the Ethics of Animal Care and Use of the Chinese Center for Disease Control and Prevention (Permit 20140509015). The study was conducted in accordance with the Guide for the Care and Use of Wild Mammals in Research of the People's Republic of China.

### Cell cultures

African green monkey kidney cells (Vero E6), human epithelial colorectal adenocarcinoma cells (CaCo-2), human epithelial type 2 HeLa derivative cells (HEp-2) and human lung carcinoma cells (A549) were purchased from the China Center for Type Culture Collection, while baby hamster kidney (BHK-21) and Madin-Darby canine kidney (MDCK) cells were obtained from the Cell Resource Center of the Shanghai Institute for Biological Sciences, Chinese Academy of Sciences. The immortalized kidney cell line of *Myotis Davidii* (IKMD) was a generous gift of Dr. Zhengli Shi, Wuhan Institute of Virology, Chinese Academy of Sciences. Cells were grown in Eagle's minimum essential medium (EMEM) (A549, BHK-21) or in Dulbecco's modified EMEM (DMEM) (Vero E6, CaCo-2, HEp-2, MDCK, IBIE and IKMD) supplemented with 10% or 20% (CaCo-2) fetal bovine serum in a humidified chamber containing 5% CO<sub>2</sub> at 37°C.

### Sample collection

All the bats analyzed here were captured at a roosting site with the assistance of villagers and staff of local the CDC office in Xishuangbanna, Yunnan Province, China. The rectal swab samples were collected and placed in the cryotube with viral transport medium (VTM) containing Earle's balanced salt solution (Invitrogen, United States), 5% bovine albumin, 50,000 µg/ml vancomycin, 50,000 µg/ml amikacin, 10,000 units/ml nystatin [51]. All samples were immediately stored in liquid nitrogen and then transported with dry ice to our laboratory in Beijing and stored in the ultra-low temperature freezer until used for RNA extraction.

### RNA extraction

Total RNA was extracted from 100 µL of VTM suspension of each swab with the RNeasy Mini Kit (Qiagen, Germany) according to the manufacturer's protocol. The RNA was eluted in 60 µL AVE buffer, of which 8 µL RNA was used as the template for RT-PCR immediately, or stored at −80°C until use.

### Pan-coronavirus RT-PCR

Total RNA extracted from the rectal swab suspension was screened for the presence of coronavirus RNA using pan-coronavirus RT-PCR with universal degenerate primers. The primers were designed from a highly conserved region of the RdRp (primer sequences are presented in [S4 Table](#)). After the reverse transcription and synthesization of cDNA with SuperScript III Reverse Transcriptase (Invitrogen, United States), a semi-nested PCR was performed. The expected amplicons of two rounds were 299 bp (using primers panCoV<sub>s</sub>-OF and panCoV<sub>s</sub>-OR) and 228 bp (using primers panCoV<sub>s</sub>-IF and panCoV<sub>s</sub>-OR) in length, respectively. All positive results were repeated and confirmed with fresh RNA extracts from the original bat rectal swab suspensions. Purified DNA amplicons (both rounds) were sequenced bi-directionally with pan-coronavirus sequencing primers ([S4 Table](#)) on an ABI Prism 3730 automated capillary sequencer (Applied Biosystems, United States).

## Complete genome sequencing

Fresh RNA was extracted from sample numbers 346 and 356 which were confirmed as coronavirus positive. The RNA were subjected to Next Generation Sequencing (NGS) using the Ion Proton platform. The original NGS data were filtered, refined and mapped to the reference sequence of Ro-BatCoV HKU9 (GenBank accession number NC\_009021) using SOAP (Short Oligonucleotide Alignment Program) [52]. Any remaining gaps in the genome were closed by PCR amplification of these regions with specific primers and then sequenced. Complete genome sequences were confirmed with Sanger sequencing on the fragments amplified with a set of primers that covered the whole genome. The 5'- and 3'-RACE analyses were performed with 5'- and 3'- Full RACE Kit (Takara, Japan) according to the manufacturer's instructions.

## Genome analyses

As the amplification of 5'-end of the genome of Ro-BatCoV GCCDC1 strain 346 was unsuccessful, we focused our genome analyses on the complete genome of Ro-BatCoV GCCDC1 strain 356. This genome was compared to those of eight complete genomes of Ro-BatCoV HKU9 (GenBank accession numbers NC\_009021, EF065514, EF065515, EF065516, HM211098, HM211099, HM211100 and HM211101, respectively) to annotate the 1ab, S, NS3, E, M and N ORFs, respectively. As the origin of the ORFs at the 3'-end of the genome were uncertain they were also blasted (tblastx) against the GenBank database. The amino acid sequence of ORF1ab was aligned with the reference sequences of SARS-CoV, human coronavirus HKU1, infectious bronchitis virus, turkey coronavirus, bovine coronavirus, mouse hepatitis virus and porcine epidemic diarrhea virus (GenBank accession numbers NC\_004718, NC\_006577, NC\_001451, NC\_010800, NC\_003045, NC\_001846 and NC\_003436, respectively) to determine the cleavage and recognition patterns of the C-like proteinase and papain-like proteinase of the 16 nonstructural proteins. In addition, the sequences of the 5' untranslated region (5'-UTR) and 3' untranslated region (3'-UTR) were defined, and the leader sequence, the leader and body TRSs were illustrated, based on comparison with SARS-CoV.

## Confirmation of the p10 gene

To eliminate the possibility of false amplification of DNA polymerase or inaccurate assembly of NGS data, the raw NGS data were further scrutinized and reads extracted for mapping to check the continuity of the p10 sequence, especially the upstream junction site between N and p10 genes and the downstream junction site between the p10 and NS7a genes. In addition, two sets of specific primers were designed to confirm the integrity and continuity of sequence surrounding the p10 gene (primer sequences shown in [S5 Table](#)). The amplicons were subsequently cloned into the pMD18-T vector and recombinant plasmids were subjected to Sanger sequencing.

## Phylogenetic analyses

To determine the phylogenetic position of the newly identified coronavirus among the known diversity of coronaviruses, the amino acid sequences of the RdRp, S, and N proteins were used for phylogenetic analyses (GenBank accession numbers shown in [S2 Table](#)). In the case of the imported p10 gene, homologous sequences of orthoreoviruses were utilized as the background data set in the phylogenetic analysis (GenBank accession numbers listed in [S3 Table](#)). All amino acid sequences were aligned using MUSCLE [53], and all poorly or ambiguously aligned regions were removed using GBLOCKS [54]. Because of the short length of the p10 and N amino acid sequence alignments, more relaxed GBLOCKS parameters were used in these cases. In all

cases phylogenetic trees of amino acid sequence alignments were inferred using the maximum likelihood method available in the PhyML package [55], with bootstrap values estimated from 1,000 replicate trees. Each tree was inferred using the LG model of amino acid substitution with values of the gamma shape parameter inferred using ProtTest [56]. Finally, all phylogenetic trees were displayed and annotated with FigTree.

## Virus culture and attempted virus isolations

Samples positive for coronavirus were cultured in Vero E6, BHK-21, MDCK, A549, HEp-2, CaCo-2 cells, as well as in an immortalized kidney cell line of *Myotis Davidii*. The cell lines were inoculated with positive samples and three blind passages were performed for each sample. The culture supernatant and cell pellet of each passage were harvested. The detection of viral replication was conducted using specific primers targeting the conserved region of RdRp.

## Subgenome identification and sequencing

Nested subgenomic mRNAs are generated during the replication cycle of coronaviruses. Hence, the identification of subgenomic mRNAs in the samples provides strong evidence for the replication of coronavirus. To analyze the possibility of replication in the newly identified bat coronavirus, primers were designed to determine the presence of viral subgenomic mRNAs in the coronavirus-positive bat rectal swab samples. Forward primers were designed targeting the leader sequence at the 5'-end of the complete genome and the putative subgenomic mRNAs, while reverse primers were designed within the ORFs or downstream of the corresponding gene (primer sequences are shown in [S6 Table](#)). Specific amplicons, that matched the expected length, were purified and then cloned into the pMD-18T vector for sequencing, while the additional suspected bands on the agarose gels were excised, purified, and then subjected to direct sequencing. Since the specific amplicon of subgenomic mRNA NS7c failed to be cloned into the vectors, the PCR product was used as a template for a second round of nested PCR. The product was then confirmed with agarose gel electrophoresis and the band was cloned for sequencing.

## p10 antiserum production

The protein family of the putative p10 protein was analyzed using PFAM [57] and InterProScan [58]. Prediction of transmembrane domains was performed using TMHMM [59], TMPred and PredictProtein [60]. Peptides corresponding to the ectodomain (from amino acid positions 2–37) and the cytoplasmic domain (the last 33 amino acids) (peptide sequences are described in [S7 Table](#)) of the putative p10 protein were synthesized (Xuheyuan Biological Technology Co., LTD, Beijing, China). After conjugation with keyhole limpet hemocyanin (KLM), the synthesized peptides were used to immunize mice for antibody production. The mice (five mice per peptide) were injected intramuscularly at their hind legs with 20 µg of the conjugated peptide mixed with adjuvant, followed by boosts until 14 days with the same conjugated peptides. Seven days after the boosts, the mice were killed and their blood collected to isolate sera. Antibody titers were determined using enzyme-linked immunosorbent assay (ELISA).

## Syncytial analysis and cell staining

In the cells infected with avian- or bat-origin fusogenic orthoreoviruses, the formation of cell syncytia depends on a p10 protein, which is encoded by the first ORF in segment S1 of the reovirus genome. It was previously demonstrated that amino acid residues of p10 proteins could be sorted into absolutely, highly, moderately and non-conserved amino acids [26].



Sequence and phylogenetic analyses indicated that the p10 gene of Ro-BatCoV GCCDC1 most likely originated in an orthoreovirus. Comparative sequence analysis revealed that although the majority of key amino acids and motifs of the Ro-BatCoV GCCDC1 p10 protein were conserved, there were 8 amino acids differences (including 2 deletions) among the 28 so-called 'absolutely conserved' amino acids that characterize members of the FAST family (Fig 7). Hence, it is necessary to explore the potential role of the p10 gene during the life cycle of Ro-BatCoV GCCDC1.

To determine whether the putative p10 protein could play the same role as homologous proteins of avian and bat orthoreoviruses, the p10 gene was cloned into the pCAGGS vector and the recombinant plasmid (Fig 8A) was then transfected into BHK-21 cells using Polyethylimine (PEI, Polysciences Inc.) according to the manufacturer's protocol. At the appropriate time post-transfection, cell-to-cell fusion was observed for the syncytium formation under the light microscope using Wright-Giemsa staining and an indirect immunofluorescence assay employing the polyclonal antibodies prepared above. The p10 gene of Pulau virus, a bat orthoreovirus [49], was also cloned into the pCAGGS vector to serve as a positive control. Cells transfected with an empty pCAGGS vector were used as a mock control.

The next step is to confirm that p10 can be transcribed or translated during the replication cycle of Ro-BatCoV GCCDC1. We confirmed that the p10 gene could be transcribed from the genome during the replication cycle of Ro-BatCoV GCCDC1, with the p10 subgenomic mRNA representing a distinct signal. Further, we cloned the deduced p10 subgenome into a pcDNA3.0-derived vector to construct an artificial plasmid (Fig 8C), which could be transcribed out of an mRNA that is consistent with the p10 subgenomic mRNA in the infected cells of the host. The recombinant plasmid was transfected into BHK-21 cells and cell syncytia were observed as described above. The recombinant plasmid of Pulau virus p10 gene was still served as positive control. Cells transfected with empty pcDNA3.0 vector were used as mock control.

## Mutational analysis of the p10 protein of Ro-BatCoV GCCDC1

As the p10 protein of Ro-BatCoV GCCDC1 is the first reported in an enveloped virus, we first tried to define the key amino acids for the p10 protein in the Ro-BatCoV GCCDC1 as described previously for p10 protein of reoviruses [24, 25]. For syncytial indexing of six mutant constructs, each well of BHK-21 monolayer cells in a 6-well plate were transfected with 2 µg of plasmid DNA using Polyethylimine (PEI, Polysciences Inc.) and incubated for 5 h before replacing the transfection mixture with DMEM growth media (Invitrogen) supplemented with 10% fetal bovine serum (GIBCO). Transfected cells were paraformaldehyde-fixed and stained with Wright-Giemsa at the indicated times, and syncytia were observed and pictures were taken at ×100 magnification on an Olympus IX51FL+DP70 microscope.

## Western blotting (WB)

The original specimens of bat rectal swabs and feces were used to test the expression of p10. BHK-21 cells with transient expression plasmid of p10 gene (pCAGGS-p10) were used as a positive control. Briefly, bat specimens and BHK-21 cell lysates were subjected to SDS-PAGE and transferred to a PVDF membrane. The membranes were blocked with a 5% non-fat dry milk solution and incubated with p10 antibody overnight at 4°C followed by peroxidase-conjugated affinipure goat anti-mouse IgG (H+L) (Zhongshan Goldenbridge, Beijing). After washing with TBS-T buffer, the membrane was treated with Immobilon™ Western Chemiluminescent HRP Substrate (Millipore, Billerica) and pictures were taken with Chemiluminescence System MicroChemi 4.2 (DNR Bio-Imaging Systems Ltd, USA).



## Accession numbers

The complete genome sequences of Ro-BatCoV GCCDC1 strains 346 and 356 have been deposited in the GenBank database and assigned accession numbers KU762337 and KU762338, respectively. We also deposited the sequences of the p10 genes from the rectal swabs of 24 bats in GenBank. All these accession numbers are listed in [S8 Table](#).

## Supporting Information

**S1 Fig. Identification of p10 gene with raw NGS data.** The READs were extracted from the raw NGS data and then mapped to the complete genome of Ro-BatCoV GCCDC1 using Genious R9 (Biomatters Limited) to confirm the integrity and continuity of context sequence surrounding the p10 gene, especially the upstream junction site between N and p10 genes, and downstream junction site between p10 and NS7a genes.

(TIF)

**S2 Fig. Comparison of 3'-end of the coronavirus genomes from group D in the genus *Beta-coronavirus*.** The TRSs of NS7a or ORF<sub>x</sub> gene just downstream of the N gene are marked with red arrows. The length of intergenic spacer between N gene and NS7a or ORF<sub>x</sub> gene is indicated with numbers. GenBank accession numbers of the coronaviruses used in this analysis: Ro-BatCoV HKU9: Roussettus bat coronavirus HKU9 (NC\_009021, EF065514, EF065515, EF065516, HM211098, HM211099, HM211100, HM211101); BatCoV philippines: Bat coronavirus Philippines/Diliman1525G2/2008 (AB543561); Ei-BatCoV Kenya: Eidolon bat coronavirus/Kenya/KY24/2006 (HQ728482); Ro-BatCoV Kenya: Roussettus bat coronavirus/Kenya/KY06/2006 (HQ728483).

(TIF)

**S3 Fig. Sequencing of subgenomic mRNAs and the identification of TRS.** Amplicon of each subgenomic mRNA, including S, NS3, E, M, N, p10, NS7a, NS7b and NS7c, was sequenced and illustrated with sequencing peak pattern. The leader sequence, TRS and CDS are marked with blue, red and yellow arrow respectively. The bias of TRS of p10 gene is marked with a yellow block.

(TIF)

**S4 Fig. Cell syncytia with images stained DAPI and with merged images.** (A) Transient expression of p10 gene and syncytium formation. **First row:** cells were stained with DAPI. **Second row:** the merged image. (From the second to the fourth row, stained monolayers were imaged using a Nikon DIAPHOT-TMD under 200× magnification. Scale bars = 50 μm). (B) Transient expression of p10 gene and syncytium formation with recombinant subgenomic p10 plasmid. **First row:** cells were stained with DAPI. **Second row:** the merged image. (From the second to forth row, stained monolayers were imaged using a Nikon DIAPHOT-TMD under 200× magnification. Scale bars = 50 μm).

(TIF)

**S5 Fig. Functionality of p10 in Ro-BatCoV GCCDC1 depends on traditional conserved domains relevant for membrane fusion.** (A) Schematic representation of p10 protein and mutant constructs. The substituted and inserted amino acids were marked with yellow and green blocks respectively. Motifs presented in the ectodomain (HP, hydrophobic patch; CM, conserved motif), endodomain (PB, polybasic) and the central transmembrane domain (TMD) are depicted with yellow rectangles. The four conserved cysteine residues (C) are shown. The two cysteines in the ectodomain form an intra-molecular disulfide bond. (B) Transient expression and the observation of syncytium formation on the monolayer BHK-21 cells transfected

with recombinant plasmid of wild type of Ro-BatCoV GCCDC1 p10 gene, mutant constructs and empty pCAGGS vector. (Wright-Giemsa staining: stained monolayers were imaged using an Olympus IX51FL+DP70 microscope under 100× magnification, scale bars = 200 μm). (TIF)

**S6 Fig. Physiologically expression of p10 by Ro-BatCoV GCCDC1 virus.** The expression of p10 protein are observed in fecal samples revealed by Western blotting. Rectal Swab 118: Representative of the samples which are negative for the Ro-BatCoV GCCDC1 RNA test. BHK21-p10: BHK-21 cells transfected with transient expression plasmid of p10 gene (pCAGGS-p10) as positive control. Feces 341 and 348: Feces samples of representatives of the feces samples whose corresponding rectal swabs are positive for the Ro-BatCoV GCCDC1 RNA test. Con. Swabs: The concentrated sample of 47 swabs which are positive for the Ro-BatCoV GCCDC1 RNA test. (TIF)

**S1 Table. Comparison of accessory genes at the 3'-end of Ro-BatCoV GCCDC1 genome of with those of Ro-BatCoV HKU9 strains and other related bat coronaviruses.** (DOCX)

**S2 Table. The selected coronaviruses and related GenBank accession numbers used in the construction of phylogenetic trees of RdRp, Spike and Nucleocapsid proteins.** (DOCX)

**S3 Table. The selected orthoreoviruses and related GenBank accession numbers used in the construction of phylogenetic tree of p10 protein.** (DOCX)

**S4 Table. Universal degenerate primers for pan-coronavirus RT-PCR and primers for sequencing.** (DOCX)

**S5 Table. Primers for the confirmation of integrity and continuity of context sequence surrounding the p10 gene.** (DOCX)

**S6 Table. Primers for the detection of viral subgenomic mRNAs.** (DOCX)

**S7 Table. Peptides of putative p10 protein for antibody production.** (DOCX)

**S8 Table. The sequences and accession numbers in this study.** (DOCX)

**S1 File. The reads of p10 in raw data of NGS.** (RAR)

**S2 File. Confirmation of p10 gene by cloning.** (RAR)

## Acknowledgments

We are grateful to Dr. Xiaojuan Guo and Dr. Xiaohui Zou from the National Institute for Viral Disease Control and Prevention, Chinese Center for Disease Control and Prevention, for their assistance in taking pictures of syncytium formation. We thank Dr. Yang Yang and Professor

Wenjie Tan from the National Institute for Viral Disease Control and Prevention, Chinese Center for Disease Control and Prevention for providing the pcDNA3.0 derivate vector. We thank all the villagers and the staff of local CDC offices in Xishuangbanna, Yunnan Province, China, for their assistance in sample collection. We thank the staff of Beijing Genomics Institute (BGI-Shenzhen, China) for the assistance of next-generation sequencing and data analysis. Finally, we thank Dr. Zhengli Shi from Wuhan Institute of Virology, Chinese Academy of Sciences, for her generous gift of the immortalized kidney cell line of *Myotis Davidii*.

## Author Contributions

**Conceptualization:** LL GFG.

**Formal analysis:** CH WJL WX TJ QW LW DL GL.

**Funding acquisition:** HY LL GFG.

**Investigation:** CH WJL WX YZha JS WJ HJ YZho HW HZ HLi HLi.

**Project administration:** CH WJL LL GFG.

**Resources:** WX HY LL.

**Supervision:** LL GFG.

**Writing – original draft:** CH WJL YS YW LL GFG.

**Writing – review & editing:** CH WJL ECH GFG.

## References

1. Knipe DM, Howley PM. Fields virology. 6th ed. Philadelphia, PA: Wolters Kluwer/Lippincott Williams & Wilkins Health; 2013. 2 volumes p.825–58.
2. King AMQ, Adams MJ, Carstens EB, Lefkowitz EJ. Virus taxonomy: classification and nomenclature of viruses: ninth report of the International Committee on Taxonomy of Viruses. London; Waltham, MA: Academic Press; 2012. x, 1327 p. p. 806–28.
3. Woo PC, Lau SK, Lam CS, Lai KK, Huang Y, Lee P, et al. Comparative analysis of complete genome sequences of three avian coronaviruses reveals a novel group 3c coronavirus. J Virol. 2009; 83(2):908–17. doi: [10.1128/JVI.01977-08](https://doi.org/10.1128/JVI.01977-08) PMID: [18971277](https://pubmed.ncbi.nlm.nih.gov/18971277/); PubMed Central PMCID: PMCPMC2612373.
4. Makino S, Keck JG, Stohlman SA, Lai MM. High-frequency RNA recombination of murine coronaviruses. J Virol. 1986; 57(3):729–37. Epub 1986/03/01. PMID: [3005623](https://pubmed.ncbi.nlm.nih.gov/3005623/); PubMed Central PMCID: PMCPmc252799.
5. Lai MM, editor Recombination in large RNA viruses: coronaviruses. Semin Virol; 1996; 7(6):381–388.
6. Woo PC, Lau SK, Huang Y, Yuen KY. Coronavirus diversity, phylogeny and interspecies jumping. Exp Biol Med (Maywood). 2009; 234(10):1117–27. doi: [10.3181/0903-MR-94](https://doi.org/10.3181/0903-MR-94) PMID: [19546349](https://pubmed.ncbi.nlm.nih.gov/19546349/).
7. Ksiazek TG, Erdman D, Goldsmith CS, Zaki SR, Peret T, Emery S, et al. A novel coronavirus associated with severe acute respiratory syndrome. N Engl J Med. 2003; 348(20):1953–66. doi: [10.1056/NEJMoa030781](https://doi.org/10.1056/NEJMoa030781) PMID: [12690092](https://pubmed.ncbi.nlm.nih.gov/12690092/).
8. Drosten C, Gunther S, Preiser W, van der Werf S, Brodt HR, Becker S, et al. Identification of a novel coronavirus in patients with severe acute respiratory syndrome. N Engl J Med. 2003; 348(20):1967–76. doi: [10.1056/NEJMoa030747](https://doi.org/10.1056/NEJMoa030747) PMID: [12690091](https://pubmed.ncbi.nlm.nih.gov/12690091/).
9. Rota PA, Oberste MS, Monroe SS, Nix WA, Campagnoli R, Icenogle JP, et al. Characterization of a novel coronavirus associated with severe acute respiratory syndrome. Science. 2003; 300(5624):1394–9. doi: [10.1126/science.1085952](https://doi.org/10.1126/science.1085952) PMID: [12730500](https://pubmed.ncbi.nlm.nih.gov/12730500/).
10. Su S, Wong G, Shi W, Liu J, Lai AC, Zhou J, et al. Epidemiology, Genetic Recombination, and Pathogenesis of Coronaviruses. Trends Microbiol. 2016; 24(6):490–502. doi: [10.1016/j.tim.2016.03.003](https://doi.org/10.1016/j.tim.2016.03.003) PMID: [27012512](https://pubmed.ncbi.nlm.nih.gov/27012512/).
11. Corman VM, Baldwin HJ, Tateno AF, Zerbinati RM, Annan A, Owusu M, et al. Evidence for an Ancestral Association of Human Coronavirus 229E with Bats. J Virol. 2015; 89(23):11858–70. Epub 2015/09/18. doi: [10.1128/jvi.01755-15](https://doi.org/10.1128/jvi.01755-15) PMID: [26378164](https://pubmed.ncbi.nlm.nih.gov/26378164/); PubMed Central PMCID: PMCPmc4645311.

12. Ge XY, Li JL, Yang XL, Chmura AA, Zhu G, Epstein JH, et al. Isolation and characterization of a bat SARS-like coronavirus that uses the ACE2 receptor. *Nature*. 2013; 503(7477):535–8. doi: [10.1038/nature12711](https://doi.org/10.1038/nature12711) PMID: [24172901](https://pubmed.ncbi.nlm.nih.gov/24172901/).
13. Corman VM, Ithete NL, Richards LR, Schoeman MC, Preiser W, Drosten C, et al. Rooting the phylogenetic tree of middle East respiratory syndrome coronavirus by characterization of a conspecific virus from an African bat. *J Virol*. 2014; 88(19):11297–303. doi: [10.1128/JVI.01498-14](https://doi.org/10.1128/JVI.01498-14) PMID: [25031349](https://pubmed.ncbi.nlm.nih.gov/25031349/); PubMed Central PMCID: PMC4178802.
14. Wang Q, Qi J, Yuan Y, Xuan Y, Han P, Wan Y, et al. Bat origins of MERS-CoV supported by bat coronavirus HKU4 usage of human receptor CD26. *Cell Host Microbe*. 2014; 16(3):328–37. doi: [10.1016/j.chom.2014.08.009](https://doi.org/10.1016/j.chom.2014.08.009) PMID: [25211075](https://pubmed.ncbi.nlm.nih.gov/25211075/).
15. Shi Z. Bat and virus. *Protein Cell*. 2010; 1(2):109–14. Epub 2011/01/05. doi: [10.1007/s13238-010-0029-7](https://doi.org/10.1007/s13238-010-0029-7) PMID: [21203979](https://pubmed.ncbi.nlm.nih.gov/21203979/).
16. Smith I, Wang LF. Bats and their virome: an important source of emerging viruses capable of infecting humans. *Curr Opin Virol*. 2013; 3(1):84–91. Epub 2012/12/26. doi: [10.1016/j.coviro.2012.11.006](https://doi.org/10.1016/j.coviro.2012.11.006) PMID: [23265969](https://pubmed.ncbi.nlm.nih.gov/23265969/).
17. Wu Y, Wu Y, Tefsen B, Shi Y, Gao GF. Bat-derived influenza-like viruses H17N10 and H18N11. *Trends Microbiol*. 2014; 22(4):183–91. doi: [10.1016/j.tim.2014.01.010](https://doi.org/10.1016/j.tim.2014.01.010) PMID: [24582528](https://pubmed.ncbi.nlm.nih.gov/24582528/).
18. Woo PC, Wang M, Lau SK, Xu H, Poon RW, Guo R, et al. Comparative analysis of twelve genomes of three novel group 2c and group 2d coronaviruses reveals unique group and subgroup features. *J Virol*. 2007; 81(4):1574–85. doi: [10.1128/JVI.02182-06](https://doi.org/10.1128/JVI.02182-06) PMID: [17121802](https://pubmed.ncbi.nlm.nih.gov/17121802/); PubMed Central PMCID: PMC1797546.
19. Drexler JF, Gloza-Rausch F, Glende J, Corman VM, Muth D, Goettsche M, et al. Genomic characterization of severe acute respiratory syndrome-related coronavirus in European bats and classification of coronaviruses based on partial RNA-dependent RNA polymerase gene sequences. *J Virol*. 2010; 84(21):11336–49. doi: [10.1128/JVI.00650-10](https://doi.org/10.1128/JVI.00650-10) PMID: [20686038](https://pubmed.ncbi.nlm.nih.gov/20686038/); PubMed Central PMCID: PMC2953168.
20. Ciechomska M, Duncan R. Reovirus FAST proteins: virus-encoded cellular fusogens. *Trends Microbiol*. 2014; 22(12):715–24. Epub 2014/09/24. doi: [10.1016/j.tim.2014.08.005](https://doi.org/10.1016/j.tim.2014.08.005) PMID: [25245455](https://pubmed.ncbi.nlm.nih.gov/25245455/).
21. Tamura K, Stecher G, Peterson D, Filipinski A, Kumar S. MEGA6: Molecular Evolutionary Genetics Analysis version 6.0. *Mol Biol Evol*. 2013; 30(12):2725–9. doi: [10.1093/molbev/mst197](https://doi.org/10.1093/molbev/mst197) PMID: [24132122](https://pubmed.ncbi.nlm.nih.gov/24132122/); PubMed Central PMCID: PMC3840312.
22. Gao F, Ou HY, Chen LL, Zheng WX, Zhang CT. Prediction of proteinase cleavage sites in polyproteins of coronaviruses and its applications in analyzing SARS-CoV genomes. *FEBS Lett*. 2003; 553(3):451–6. Epub 2003/10/24. doi: [S0014579303010913](https://doi.org/S0014579303010913) [pii]. PMID: [14572668](https://pubmed.ncbi.nlm.nih.gov/14572668/).
23. Fang S, Shen H, Wang J, Tay FP, Liu DX. Functional and genetic studies of the substrate specificity of coronavirus infectious bronchitis virus 3C-like proteinase. *J Virol*. 2010; 84(14):7325–36. doi: [10.1128/JVI.02490-09](https://doi.org/10.1128/JVI.02490-09) PMID: [20444893](https://pubmed.ncbi.nlm.nih.gov/20444893/); PubMed Central PMCID: PMC2898227.
24. Shmulevitz M, Epand RF, Epand RM, Duncan R. Structural and functional properties of an unusual internal fusion peptide in a nonenveloped virus membrane fusion protein. *J Virol*. 2004; 78(6):2808–18. Epub 2004/03/03. PMID: [14990700](https://pubmed.ncbi.nlm.nih.gov/14990700/); PubMed Central PMCID: PMC353762.
25. Barry C, Key T, Haddad R, Duncan R. Features of a spatially constrained cystine loop in the p10 FAST protein ectodomain define a new class of viral fusion peptides. *J Biol Chem*. 2010; 285(22):16424–33. Epub 2010/04/07. doi: [10.1074/jbc.M110.118232](https://doi.org/10.1074/jbc.M110.118232) PMID: [20363742](https://pubmed.ncbi.nlm.nih.gov/20363742/); PubMed Central PMCID: PMC2878076.
26. Key T, Duncan R. A compact, multifunctional fusion module directs cholesterol-dependent homomultimerization and syncytiogenic efficiency of reovirus p10 FAST proteins. *PLoS Pathog*. 2014; 10(3):e1004023. doi: [10.1371/journal.ppat.1004023](https://doi.org/10.1371/journal.ppat.1004023) PMID: [24651689](https://pubmed.ncbi.nlm.nih.gov/24651689/); PubMed Central PMCID: PMC3961370.
27. Stavrinides J, Guttman DS. Mosaic evolution of the severe acute respiratory syndrome coronavirus. *J Virol*. 2004; 78(1):76–82. PMID: [14671089](https://pubmed.ncbi.nlm.nih.gov/14671089/); PubMed Central PMCID: PMC303383.
28. Terada Y, Matsui N, Noguchi K, Kuwata R, Shimoda H, Soma T, et al. Emergence of pathogenic coronaviruses in cats by homologous recombination between feline and canine coronaviruses. *PLoS One*. 2014; 9(9):e106534. doi: [10.1371/journal.pone.0106534](https://doi.org/10.1371/journal.pone.0106534) PMID: [25180686](https://pubmed.ncbi.nlm.nih.gov/25180686/); PubMed Central PMCID: PMC4152292.
29. Wang Y, Liu D, Shi W, Lu R, Wang W, Zhao Y, et al. Origin and Possible Genetic Recombination of the Middle East Respiratory Syndrome Coronavirus from the First Imported Case in China: Phylogenetics and Coalescence Analysis. *mBio*. 2015; 6(5):e01280–15. doi: [10.1128/mBio.01280-15](https://doi.org/10.1128/mBio.01280-15) PMID: [26350969](https://pubmed.ncbi.nlm.nih.gov/26350969/); PubMed Central PMCID: PMC4600111.

30. Luytjes W, Bredenbeek PJ, Noten AF, Horzinek MC, Spaan WJ. Sequence of mouse hepatitis virus A59 mRNA 2: indications for RNA recombination between coronaviruses and influenza C virus. *Virology*. 1988; 166(2):415–22. PMID: [2845655](#).
31. Zhang XM, Kousoulas KG, Storz J. The hemagglutinin/esterase gene of human coronavirus strain OC43: phylogenetic relationships to bovine and murine coronaviruses and influenza C virus. *Virology*. 1992; 186(1):318–23. Epub 1992/01/01. PMID: [1727608](#).
32. Cornelissen LA, Wierda CM, van der Meer FJ, Herrewegh AA, Horzinek MC, Egberink HF, et al. Hemagglutinin-esterase, a novel structural protein of torovirus. *J Virol*. 1997; 71(7):5277–86. PMID: [9188596](#); PubMed Central PMCID: PMC191764.
33. Gibbs MJ, Weiller GF. Evidence that a plant virus switched hosts to infect a vertebrate and then recombined with a vertebrate-infecting virus. *Proc Natl Acad Sci U S A*. 1999; 96(14):8022–7. PMID: [10393941](#); PubMed Central PMCID: PMC1922181.
34. Woolford L, Rector A, Van Ranst M, Ducki A, Bennett MD, Nicholls PK, et al. A novel virus detected in papillomas and carcinomas of the endangered western barred bandicoot (*Perameles bougainville*) exhibits genomic features of both the Papillomaviridae and Polyomaviridae. *J Virol*. 2007; 81(24):13280–90. doi: [10.1128/JVI.01662-07](#) PMID: [17898069](#); PubMed Central PMCID: PMC1922181.
35. Davidson I, Borenshtain R. In vivo events of retroviral long terminal repeat integration into Marek's disease virus in commercial poultry: detection of chimeric molecules as a marker. *Avian Dis*. 2001; 45(1):102–21. PMID: [11332471](#).
36. Singh P, Schnitzlein WM, Tripathy DN. Reticuloendotheliosis virus sequences within the genomes of field strains of fowlpox virus display variability. *J Virol*. 2003; 77(10):5855–62. PMID: [12719579](#); PubMed Central PMCID: PMC1922181.
37. Brown CW, Stephenson KB, Hanson S, Kucharczyk M, Duncan R, Bell JC, et al. The p14 FAST protein of reptilian reovirus increases vesicular stomatitis virus neuropathogenesis. *J Virol*. 2009; 83(2):552–61. Epub 2008/10/31. doi: [10.1128/jvi.01921-08](#) PMID: [18971262](#); PubMed Central PMCID: PMC1922181.
38. de Groot RJ. Structure, function and evolution of the hemagglutinin-esterase proteins of corona- and toroviruses. *Glycoconj J*. 2006; 23(1–2):59–72. doi: [10.1007/s10719-006-5438-8](#) PMID: [16575523](#).
39. Huang X, Dong W, Milewska A, Golda A, Qi Y, Zhu QK, et al. Human Coronavirus HKU1 Spike Protein Uses O-Acetylated Sialic Acid as an Attachment Receptor Determinant and Employs Hemagglutinin-Esterase Protein as a Receptor-Destroying Enzyme. *J Virol*. 2015; 89(14):7202–13. doi: [10.1128/JVI.00854-15](#) PMID: [25926653](#); PubMed Central PMCID: PMC4473545.
40. Chua KB, Crameri G, Hyatt A, Yu M, Tompang MR, Rosli J, et al. A previously unknown reovirus of bat origin is associated with an acute respiratory disease in humans. *Proc Natl Acad Sci U S A*. 2007; 104(27):11424–9. Epub 2007/06/27. doi: [10.1073/pnas.0701372104](#) PMID: [17592121](#); PubMed Central PMCID: PMC1922181.
41. Chua KB, Voon K, Crameri G, Tan HS, Rosli J, McEachern JA, et al. Identification and characterization of a new orthoreovirus from patients with acute respiratory infections. *PLoS One*. 2008; 3(11):e3803. doi: [10.1371/journal.pone.0003803](#) PMID: [19030226](#); PubMed Central PMCID: PMC1922181.
42. Su S, Wong G, Liu Y, Gao GF, Li S, Bi Y. MERS in South Korea and China: a potential outbreak threat? *Lancet*. 2015; 385(9985):2349–50. doi: [10.1016/S0140-6736\(15\)60859-5](#) PMID: [26088634](#).
43. Wong G, Liu W, Liu Y, Zhou B, Bi Y, Gao GF. MERS, SARS, and Ebola: The Role of Super-Spreaders in Infectious Disease. *Cell Host Microbe*. 2015; 18(4):398–401. doi: [10.1016/j.chom.2015.09.013](#) PMID: [26468744](#).
44. Brunger AT, Adams PD, Clore GM, DeLano WL, Gros P, Grosse-Kunstleve RW, et al. Crystallography & NMR system: A new software suite for macromolecular structure determination. *Acta Crystallogr D Biol Crystallogr*. 1998; 54(Pt 5):905–21. PMID: [9757107](#).
45. Chu DK, Peiris JS, Chen H, Guan Y, Poon LL. Genomic characterizations of bat coronaviruses (1A, 1B and HKU8) and evidence for co-infections in Miniopterus bats. *J Gen Virol*. 2008; 89(Pt 5):1282–7. doi: [10.1099/vir.0.83605-0](#) PMID: [18420807](#).
46. Wu Z, Yang L, Ren X, He G, Zhang J, Yang J, et al. Deciphering the bat virome catalog to better understand the ecological diversity of bat viruses and the bat origin of emerging infectious diseases. *ISME J*. 2016; 10(3):609–20. doi: [10.1038/ismej.2015.138](#) PMID: [26262818](#); PubMed Central PMCID: PMC1922181.
47. Hu T, Qiu W, He B, Zhang Y, Yu J, Liang X, et al. Characterization of a novel orthoreovirus isolated from fruit bat, China. *BMC Microbiol*. 2014; 14:293. Epub 2014/12/01. doi: [10.1186/s12866-014-0293-4](#) PMID: [25433675](#); PubMed Central PMCID: PMC1922181.

48. Du L, Lu Z, Fan Y, Meng K, Jiang Y, Zhu Y, et al. Xi River virus, a new bat reovirus isolated in southern China. *Arch Virol*. 2010; 155(8):1295–9. Epub 2010/05/25. doi: [10.1007/s00705-010-0690-4](https://doi.org/10.1007/s00705-010-0690-4) PMID: [20495835](https://pubmed.ncbi.nlm.nih.gov/20495835/).
49. Pritchard LI, Chua KB, Cummins D, Hyatt A, Crameri G, Eaton BT, et al. Pulau virus; a new member of the Nelson Bay orthoreovirus species isolated from fruit bats in Malaysia. *Arch Virol*. 2006; 151(2):229–39. Epub 2005/10/06. doi: [10.1007/s00705-005-0644-4](https://doi.org/10.1007/s00705-005-0644-4) PMID: [16205863](https://pubmed.ncbi.nlm.nih.gov/16205863/).
50. Duan Q, Zhu H, Yang Y, Li W, Zhou Y, He J, et al. Reovirus, isolated from SARS patients. *Chin Sci Bull*. 2003; 48(13):1293–6.
51. Lau SK, Woo PC, Li KS, Tsang AK, Fan RY, Luk HK, et al. Discovery of a novel coronavirus, China Rat-tus coronavirus HKU24, from Norway rats supports the murine origin of Betacoronavirus 1 and has implications for the ancestor of Betacoronavirus lineage A. *J Virol*. 2015; 89(6):3076–92. Epub 2015/01/02. doi: [10.1128/jvi.02420-14](https://doi.org/10.1128/jvi.02420-14) PMID: [25552712](https://pubmed.ncbi.nlm.nih.gov/25552712/); PubMed Central PMCID: [PMCPMC4337523](https://pubmed.ncbi.nlm.nih.gov/PMC4337523/).
52. Li R, Li Y, Kristiansen K, Wang J. SOAP: short oligonucleotide alignment program. *Bioinformatics*. 2008; 24(5):713–4. doi: [10.1093/bioinformatics/btn025](https://doi.org/10.1093/bioinformatics/btn025) PMID: [18227114](https://pubmed.ncbi.nlm.nih.gov/18227114/).
53. Edgar RC. MUSCLE: multiple sequence alignment with high accuracy and high throughput. *Nucleic Acids Res*. 2004; 32(5):1792–7. doi: [10.1093/nar/gkh340](https://doi.org/10.1093/nar/gkh340) PMID: [15034147](https://pubmed.ncbi.nlm.nih.gov/15034147/); PubMed Central PMCID: [PMCPMC390337](https://pubmed.ncbi.nlm.nih.gov/PMC390337/).
54. Talavera G, Castresana J. Improvement of phylogenies after removing divergent and ambiguously aligned blocks from protein sequence alignments. *Syst Biol*. 2007; 56(4):564–77. doi: [10.1080/10635150701472164](https://doi.org/10.1080/10635150701472164) PMID: [17654362](https://pubmed.ncbi.nlm.nih.gov/17654362/).
55. Guindon S, Dufayard JF, Lefort V, Anisimova M, Hordijk W, Gascuel O. New algorithms and methods to estimate maximum-likelihood phylogenies: assessing the performance of PhyML 3.0. *Syst Biol*. 2010; 59(3):307–21. doi: [10.1093/sysbio/syq010](https://doi.org/10.1093/sysbio/syq010) PMID: [20525638](https://pubmed.ncbi.nlm.nih.gov/20525638/).
56. Darriba D, Taboada GL, Doallo R, Posada D. ProtTest 3: fast selection of best-fit models of protein evolution. *Bioinformatics*. 2011; 27(8):1164–5. doi: [10.1093/bioinformatics/btr088](https://doi.org/10.1093/bioinformatics/btr088) PMID: [21335321](https://pubmed.ncbi.nlm.nih.gov/21335321/).
57. Finn RD, Bateman A, Clements J, Coggill P, Eberhardt RY, Eddy SR, et al. Pfam: the protein families database. *Nucleic Acids Res*. 2014; 42(Database issue):D222–30. doi: [10.1093/nar/gkt1223](https://doi.org/10.1093/nar/gkt1223) PMID: [24288371](https://pubmed.ncbi.nlm.nih.gov/24288371/); PubMed Central PMCID: [PMCPMC3965110](https://pubmed.ncbi.nlm.nih.gov/PMC3965110/).
58. Jones P, Binns D, Chang HY, Fraser M, Li W, McAnulla C, et al. InterProScan 5: genome-scale protein function classification. *Bioinformatics*. 2014; 30(9):1236–40. doi: [10.1093/bioinformatics/btu031](https://doi.org/10.1093/bioinformatics/btu031) PMID: [24451626](https://pubmed.ncbi.nlm.nih.gov/24451626/); PubMed Central PMCID: [PMCPMC3998142](https://pubmed.ncbi.nlm.nih.gov/PMC3998142/).
59. Krogh A, Larsson B, von Heijne G, Sonnhammer EL. Predicting transmembrane protein topology with a hidden Markov model: application to complete genomes. *J Mol Biol*. 2001; 305(3):567–80. doi: [10.1006/jmbi.2000.4315](https://doi.org/10.1006/jmbi.2000.4315) PMID: [11152613](https://pubmed.ncbi.nlm.nih.gov/11152613/).
60. Rost B, Yachdav G, Liu J. The PredictProtein server. *Nucleic Acids Res*. 2004; 32(Web Server issue):W321–6. doi: [10.1093/nar/gkh377](https://doi.org/10.1093/nar/gkh377) PMID: [15215403](https://pubmed.ncbi.nlm.nih.gov/15215403/); PubMed Central PMCID: [PMCPMC441515](https://pubmed.ncbi.nlm.nih.gov/PMC441515/).